

Università degli Studi della Calabria

**Dottorato di Ricerca in Ingegneria Chimica e dei Materiali**  
*SCUOLA DI DOTTORATO " PITAGORA " IN SCIENZE*  
*INGEGNERISTICHE*

Tesi

**Molecular modelling of imprinted  
membranes prepared by the  
noncovalent approach**

Settore Scientifico Disciplinare CHIM07 – Fondamenti chimici delle  
tecnologie

*Supervisor*

**Ch.mo Prof. Enrico DRIOLI**

**Dr. Giorgio DE LUCA**

*Candidato*

**Samuel GARCÍA DEL BLANCO**

**Ciclo XXIV**

*Il Coordinatore del Corso di Dottorato*

**Ch.mo Prof. Raffaele MOLINARI**

---

A.A. 2010-2011

A mis padres,  
Sin vosotros este sueño nunca habría sido posible. Gracias por  
todo. Os quiero.

“If I have seen further it is by standing on the shoulders of giants”.

-Sr. Isaac Newton.

# INDEX

|   |     |
|---|-----|
| <b>Preface</b>  | I   |
| <b>Prefazione</b>   | IV  |
| <b>References</b>   | VII |
| <b>Chapter 1: Theoretical Background</b>  |     |
| 1.1 Introduction  | 2   |
| 1.2 The Schrödinger Equation and Hartree-Fock Theory  | 2   |
| 1.3 The Density Functional Theory   | 3   |
| 1.4 Noncovalent interactions.   | 7   |
| 1.4.1 Hydrogen bonding  | 10  |
| 1.4.2 Electrostatic Interactions (Dipolar interactions)   | 12  |
| 1.5.3 Dispersion Interactions   | 12  |
| <b>References</b>   | 14  |
| <b>Chapter 2: Molecular Imprinting technique and membrane Technology</b>                            |     |
| 2.1 Introduction to Molecular Imprinting Technique  | 17  |
| 2.2 Membrane Technology   | 17  |
| 2.2.1 Background  | 19  |
| 2.2.2 Recent trends concerning the membrane technology  | 21  |
| 2.2.2.1 Membranes for water treatment   | 21  |
| 2.2.2.2 Membranes for chemical/biomedical applications  | 27  |
| 2.2.2.3 Membranes for Gas Separation  | 32  |
| 2.2.2.4 Membranes for environmental applications  | 36  |
| 2.3 Molecularly Imprinted Membranes (MIMs): An overview   | 37  |
| 2.3.1 MIMs preparation strategies   | 37  |
| 2.3.1.1 From pre-synthesized MIPs to MIMs   | 38  |
| 2.3.1.2 Simultaneous formation of MIP and membrane structure: Cross-linking polymerisation          | 38  |
| 2.3.1.3 Simultaneous formation of MIP and membrane structure: Polymer solution phase inversion (PI) | 38  |
| 2.3.1.4 Preparation of composite MIMs   | 40  |
| 2.3.2 MIMs Separations  | 41  |

|  |    |
|--|----|
| 2.3.2.1 Mechanisms for transport and selectivity   | 42 |
| 2.3.3 Performance of microporous MIMs  | 43 |
| 2.3.4 Macroporous MIM-MIP as affinity layer  | 43 |
| 2.3.4.1 MIP particles composited membranes   | 43 |
| 2.3.4.2 Thin layer MIP composited membranes  | 44 |
| 2.3.5 Performance of macroporous MIMs  | 44 |
| 2.3.6 Combinations of novel MIP formats with membrane separations  | 45 |
| 2.3.7 Final Remarks  | 45 |
| <b>References</b>  | 48 |
| <b>Chapter 3: Materials and Methods</b>  |    |
| 3.1 Membrane forming polymers  | 54 |
| 3.2 Target Molecules   | 55 |
| 3.3 Preparation and characterization of polymers   | 56 |
| 3.4 Preparation and characterization of flat-sheet membranes   | 57 |
| <b>References</b>  | 61 |
| <b>Chapter 4: Results and Discussion</b>   |    |
| 4.1 Computational Details  | 63 |
| 4.2 Evaluation of binding energies of the noncovalent interactions   | 64 |
| 4.3 Causes controlling the affinity of the imprinted membranes for aminic compounds                              | 71 |
| 4.4 Development of molecularly imprinted membranes for selective recognition of primary amines in organic medium | 77 |
| 4.4.1 Preparation and characterization of polymers   | 71 |
| 4.4.2 Preparation and characterization of membranes  | 79 |
| 4.4.3 Binding tests  | 81 |
| <b>References</b>  | 86 |
| <b>Conclusions and further works</b>   | 88 |
| <b>Proceedings</b>   | 92 |
| <b>Publications</b>  | 94 |

# Preface

Molecular Imprinting is today a well known and established technique applied for the recognition of specific molecules by polymeric materials. The idea of copying the specificity in many natural systems, such as enzymes or antibodies, led to the first experimental uses and subsequent improvements of this technique. The molecular imprinting is based on the interaction and subsequent spatial orientation of polymerizable functional monomers around one template molecule [1]. The polymerization confers to the supra-molecular complex rigidity and stability creating the molecularly imprinted polymers (MIPs). A soft extraction of the template molecule leaves the cavities with the shape of the template into the polymeric network. As a result, these kinds of polymers show specific molecular recognition properties and they are largely able to re-bind selectively the template discriminating between other similar molecules. In figure P.1 it is provided a general representation of the molecular imprinting.

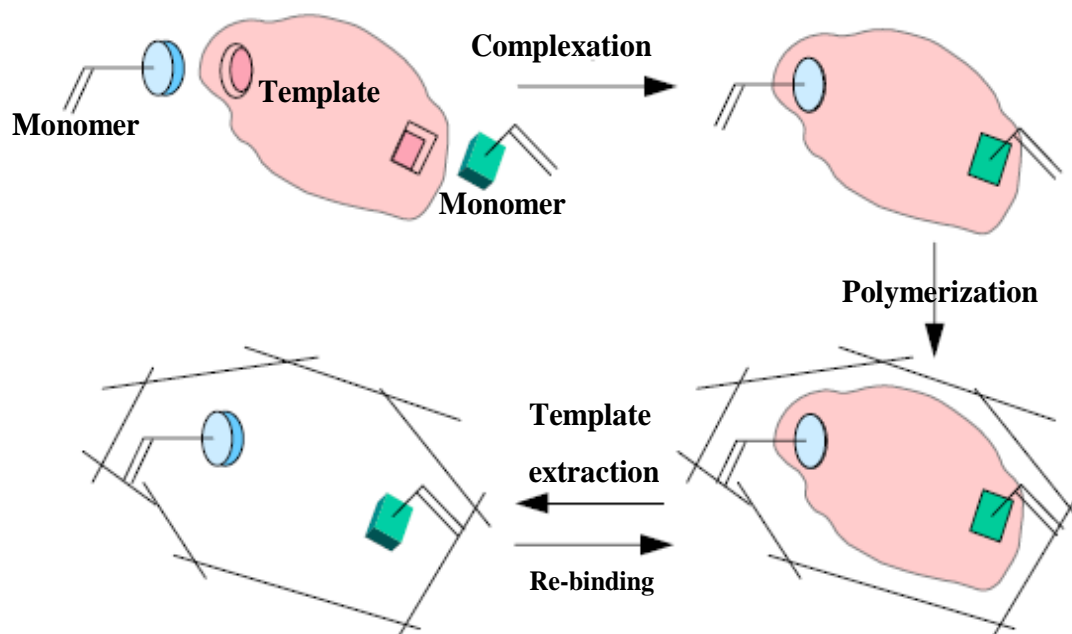


**Figure P.1:** Principle of the molecular imprinting technique.

Two main approaches of this technique were developed [2]: the covalent and non-covalent. In the covalent approach, the interaction between the template molecule and

the functional monomers occurs in a covalent manner, both in the polymerization step and in the subsequent recognition of the template. In spite of this approach gives a high selectivity, brings some disadvantages related with the limited number of monomers able to form covalent bonds with templates. Steric hindrance and an aggressive treatment for the extraction of templates are other common problems associated to this approach. As its own name indicates, the noncovalent interaction govern the assembly between template and functional monomers. The noncovalent approach is more widely used because offers a high variety of uses and the absence of a complicated synthetic chemistry in the preparation of polymers.

The combination between this technique and membrane technology led since the beginning of the 90s to the so-known as molecularly imprinted membranes (MIMs) [3]. The appearance in scene of MIMs was a cheap alternative to chromatographic methods because combine the mechanical stability of the membrane support and the specific recognition properties of MIPs materials. In spite of being a relatively young procedure, the (MIMs) technology is today one of the most applied tools in the membrane technology. However, more than 95% of the total publications about MIMs, are related with the utilisation of these in aqueous environments. This is due to the loss of the recognition efficiency of MIMs in organic solvents associated to the poor stability of the common MIMs forming materials.

In addition, there are not references in literature regarding theoretical studies, at molecular level, about the mechanism controlling the affinity of MIMs towards a particular template in organic media. Thus the scope of this PhD was the theoretical and experimental study of MIMs in organic environments.

During this PhD quantum-mechanics approach was used with the aim of acquire fundamental understanding about MIMs. Quantum mechanics calculations can help to estimate accurately some molecular chemical properties which are, currently, impossible to assess experimentally. Therefore, the theoretical knowledge acquired at the molecular level can predict and suggest novel polymeric materials to be used in the membrane technology. The work developed during this PhD can be divided in 2 areas: the experimental and theoretical part.

Concerning the experimental part, the main goal was to prepare and use molecularly imprinted membranes (MIMs) in flat-sheet configuration *via* the phase inversion technique using a noncovalent approach. The acquired experience of our institute on the use of MIMs in aqueous media [4-7], suggested us to extend their use in organic phase.

During the synthesis of most of pharmaceutical ingredients, usually, organic solvents remain polluted due to the uncompleted reaction of products utilized. The use of membranes as selective absorbers devices can help to remove some small toxic impurities such as primary aromatic amines. With the removal of these impurities, organic solvents remain cleaned and could be used again, saving energy and resources and preserving the environment.

As regards the theoretical part, the interpretation, at molecular level, of the experimental results was carried out in order to manage the experimental strategy to be used. Accurate quantum mechanics calculations were performed in the framework of Density Functional Theory (DFT). The theoretical interpretation allowed us to estimate some chemical-physical properties of the supramolecular complexes forming the MIMs, such as optimized structures and binding energies. The main goal was to understand the role of the noncovalent interactions in the impurity recognition showed by the MIMs. A comparative analysis of energies of the noncovalent interactions involved among polymeric chains and between polymeric chains with impurities was, therefore carried out. The knowledge obtained studying the noncovalent interactions can help to understand the mechanism controlling the “imprinting” phenomena in organic environments. *Ad-hoc* experiments were performed to verify the theoretical predictions. The thesis is divided in five chapters as follows:

In chapter 1, a short prologue about theoretical background of the aforementioned calculations is provided. Important information and classification of noncovalent interactions is also included here.

The chapter 2 contains a short introduction concerning the molecular imprinting technique, and an extensive background about the membrane technology including also MIMs.

The chapter 3 details carefully the preparation and characterization of the different membranes and the membranes forming polymers.

The chapter 4 includes a full discussion about the theoretical knowledge acquired as well as the different experimental results obtained. In addition, a section about computational details to explain the calculations used is also integrated.

In chapter 5 are included the conclusions and further works.



# Prefazione

Lo stampo molecolare è oggi una tecnica ben nota ed affermata usata per il riconoscimento di molecole specifiche per mezzo di materiali polimerici. L'idea di imitare la specificità presente in molti sistemi naturali, come gli enzimi ed anticorpi, diede origine ai primi usi sperimentali e successivi miglioramenti di questa tecnica [1]. Lo stampo molecolare è basato nell'interazione e successivo orientamento spaziale di diversi monomeri funzionali polimerizzabili intorno ad una molecola stampo. Dopo la formazione del complesso, la polimerizzazione che avviene, conferisce al sistema una elevata rigidità ed stabilità creando i polimeri a stampo molecolare; in inglese molecularly imprinted polymers (MIPs). La estrazione della molecola stampo dalla rete polimerica lascia cavità che hanno la sua forma specifica. Di conseguenza, questo tipo di polimeri mostrano proprietà specifiche di riconoscimento molecolare e sono, nella maggior parte dei casi, in grado di discriminare tra la molecola stampo ed altre molecole chimiche ed estrutturalmente analoghe. In figura P.1 è fornita una rappresentazione generale dello stampo molecolare.

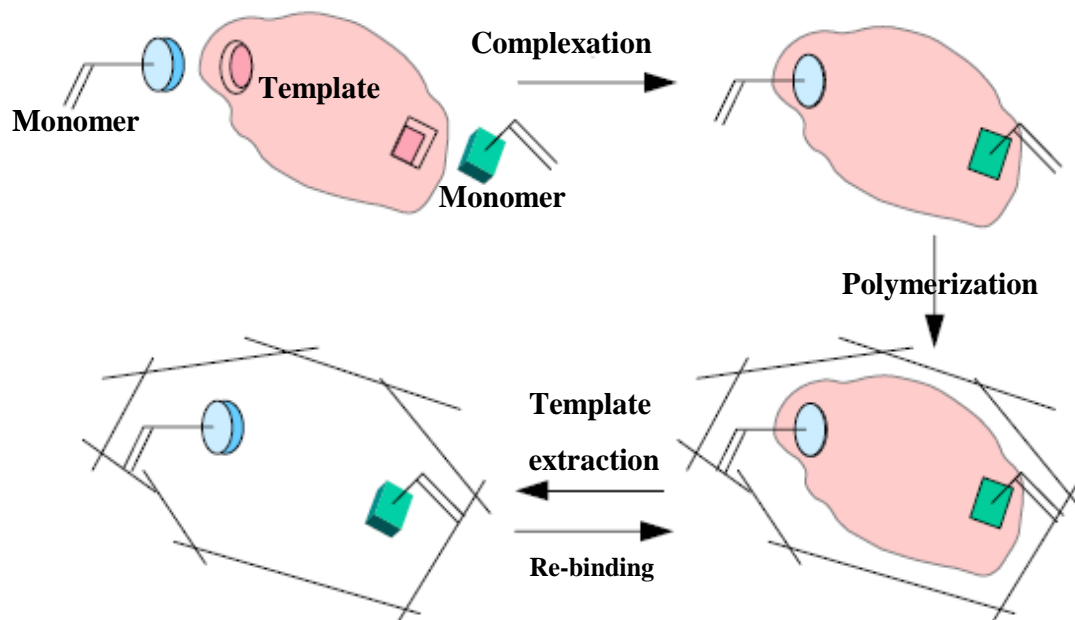


**Figure P.1:** Rappresentazione dello stampo molecolare.

Due approcci principali di questa tecnica sono stati sviluppati [2]: il covalente ed il noncovalente. Nell'approccio covalente, l'interazione tra la molecola ed i monomeri funzionali avviene in maniera covalente, sia nella fase di polimerizzazione che nella

successivo riconoscimento della molecola stampo. Nonostante questo approccio offre una elevata selectività, porta con se alcuni svantaggi associati con il numero limitato di monomeri in grado di formare legami covalenti con gli stampi. L' elevato ingombro sterico ed un trattamento troppo aggressivo per la rimozione della molecola stampo sono altri dei comuni problemi associati con questo approccio. Nell'approccio non covalente, le interazioni non covalenti, governano l'assemblaggio tra i monomeri e la molecola stampo. Questo approccio è molto più diffuso dovuto a che offre una elevata varietà di usi e la assenza di una complessa chimica sintetica per la preparazione dei polimeri. La combinazione dello stampo molecolare e la tecnologia a membrane diede origine dall'inizio degli anni 90 alle così dette membrane ad stampo molecolare; in inglese molecularly imprinted membranes (MIMs) [3]. Queste MIMs furono una reale ed economica alternativa ai metodi cromatografici esistenti in quel periodo in quanto consentivano una combinazione della stabilità meccanica del supporto di membrana con le proprietà di riconoscimento dei MIPs. Nonostante sia una metodologia relativamente recente, essa è oggi una delle più applicate nell'ambito della tecnologia a membrana. Tuttavia, più del 95% delle pubblicazioni relative a le MIMs riguardano il suo utilizzo in ambienti acquosi.

Inoltre, non ci sono riferimenti in letteratura per quanto riguarda gli studi teorici, a livello molecolare, che trattano il meccanismo che controlla l'affinità delle MIMs verso una molecola in particolare in ambienti organici. Così lo scopo di questo dottorato è stato lo studio, a livello teorico ed sperimentale delle MIMs in ambienti organici. Durante questo dottorato la meccanica quantistica è stata utilizzata con l'obiettivo di acquisire conoscenze basiche focalizzate sulle MIMs. I calcoli quantistici usati aiutarono a stimare con precisione alcune proprietà fisico-chimiche che sono, attualmente, impossibili di valutare sperimentalmente. Le conoscenze teoriche acquisite a livello molecolare sono in grado di prevedere e suggerire nuovi materiali polimerici da utilizzare dopo nella tecnologia delle MIMs. Il lavoro sviluppato nel corso di questo dottorato può essere diviso in due aree: la parte sperimentale e la parte teorica. Per quanto riguarda alla parte sperimentale, l'obiettivo principale era la preparazione e caratterizzazione di membrane a stampo molecolare (MIMs) in configurazione di foglio piatto (flat-sheet) usando la tecnica di inversione di fase con l'approccio non covalente. La esperienza acquisita nel nostro istituto con questo tipo di membrane in mezzo acquoso [4-7] ci ha suggerito di estendere il loro utilizzo anche in ambienti organici. Durante la sintesi di la maggior parte dei ingredienti farmacologici, di solito, i solventi organici

rimangono inquinati a causa della reazione incompleta dei prodotti utilizzati. L'utilizzo di MIMs come dispositivi assorbitori selettivi può aiutare a rimuovere queste impurità tossiche a volte, come per esempio, le amine aromatiche primarie (anilines). Con la rimozione di queste impurità i solventi rimangono puliti e potrebbero essere usati di nuovo, aiutando a risparmiare energia e risorse, ed in definitiva, a preservare l'ambiente.

Per quanto riguarda la parte teorica, l'interpretazione, a livello molecolare, dei risultati sperimentali è stata effettuata col fine di gestire la strategia sperimentale da utilizzare. Calcoli quantistici accurati sono stati effettuati nel ambito della teoria della Density Functional Theory (DFT). L'interpretazione teorica dei calcoli ci ha permesso di valutare alcune caratteristiche chimico-fisiche dei complessi supramolecolari che formano il MIM, come le strutture ottimizzate e energie di legame. L'obiettivo principale era quello di comprendere il ruolo delle interazioni non covalenti nel riconoscimento delle impurità mostrate dal MIM. Un'analisi comparativa delle energie delle interazioni non covalenti tra le catene polimeriche coinvolte e tra catene polimeriche con impurità è stata, quindi, effettuata. Le conoscenze acquisite studiando le interazioni non covalenti possono aiutare a capire il meccanismo di controllo dell'"imprinting" fenomeno in ambienti organici. Esperimenti *Ad-hoc* sono stati eseguiti per verificare le previsioni teoriche. La tesi è divisa in 4 capitoli come segue:

Nel capitolo 1 è fornito un breve background riguardante ai calcoli quantistici precedentemente citati. Importanti informazioni sulle interazioni noncovalenti sono anche state incluse qui.

Il capitolo 2 contiene una breve introduzione sulla tecnica dello stampo molecolare, un ampio background su la tecnologia a membrana e finalmente una parte dedicata esclusivamente alla tecnologia delle MIMs.

Il capitolo 3 descrive in dettaglio la preparazione e caratterizzazione delle membrane usate e dei diversi polimeri che formano le membrane.

Il capitolo 4 include una completa discussione sulle conoscenze teoriche acquisite ed inoltre i diversi risultati sperimentali ottenuti. Peraltro, una sezione sui dettagli computazionali per spiegare i calcoli utilizzati è pure integrata qui.

Dopo sono incluse le conclusioni finali e lavori futuri per sviluppare. Alla fine sono state aggiunte le pubblicazioni scientifiche, ed i proceedings in conferenze internazionali.

## References

- [1] Yoshikawa, M., *Biosep.* (2002) 10, 277.
- [2] Mayes, A.G., Whitcombe, M.J., *Adv. Drug. Deliv. Rev.* (2005) 57, 1742.
- [3] Wang, X.J., Xu, Z.L., Bing, N.C., Yang, Z.G., *J. Appl. Pol. Sci.* (2008) 109, 64.
- [4] Donato, L., Figoli, A., Drioli, E., *J. Pharm. Biomed. An.* (2005) 37, 1003.
- [5] Tasselli, F., Donato, L., Drioli, E., *J. Membr. Sci.* (2008) 320, 167.
- [6] Donato, L., Tasselli, F., Drioli, E., *Sep. Sci. Tech.* (2010) 45, 2273.
- [7] Donato, L., Greco, M.C., Drioli, E., *Desal. Wat. Treat.* (2011) 30, 1.

# **Chapter 1**

## **Theoretical Background**

## **1.1 Introduction**

The computational chemistry can provide a great deal of insight into a large variety of chemical systems. In fact, the computational chemistry permits to investigate properties of systems that are often inaccessible using experimental techniques. As computers with new algorithms become faster and more powerful, an increasing number of scientists are supplementing their research with computational results [1]. Computational chemistry has been widely applied in the pharmaceutical industry, as well as in the design of new materials, and it has been particularly successful in both areas. This approach can save synthetic efforts, reducing not only the material amount used but also precious manpower. As the world moves into an era of greater environmental consciousness, the optimization of resources it is being more and more a wished objective. On the other hand, computational chemistry is often used to complement experimental work, providing the detailed information needed to support experimental hypotheses [2]. In this chapter, the basic concepts of the quantum theory (Density Function Theory), used to carry out the evaluation of some molecular key properties are illustrated. In particular, the purpose of the chapter is to provide the reader with a fundamental understanding of the Density Function Theory employed during the thesis, while thorough discussions can be found in various theoretical chemistry textbooks [3-7].

One of the fundamental aspects in the study of the interface properties are the binding energies associated with noncovalent interactions involved between the functional groups constituting the interface and the permeating molecules. Thus, the last section of this chapter will explain this kind of interactions. Computational chemistry supported by the modern quantum chemistry is a very important tool useful for the evaluation of these properties.

## **1.2 The Schrödinger Equation and Hartree-Fock Theory**

In the early 20<sup>th</sup>, to accurately describe and predict the properties of atoms and molecules a new set of laws, different of classical mechanics, was needed and thus the quantum mechanics was born. These new laws accounted for the wave-particle duality of electrons, a feat that classical mechanics had failed to overcome. The laws of

quantum mechanics are extremely elegant: any microscopic system can be described by a function, known as the wave function ( $\Psi$ ). It contains all the information about the system. Very briefly, the final goal of the quantum mechanics is the determination of the correct wave function for a specific system. Unfortunately, due to the complex nature of wave function for many electrons quantum systems, an exact solution at the time it is impossible. In order to overcome this drawback several approximations and assumptions were made. Ultimately, each method discussed in this chapter employs a specific set of assumptions and as a consequence each has its own advantages and disadvantages. In quantum mechanics each observable, that is a chemical-physical property, can be described by on Hermitian operator. A representation of this operator is obtained using an appropriate set of basis in the Hilbert space, which are particle states. All the observables, that is operators, and auto functions of these operators can be represented using a particular set of basis (complete set). The value of a chemical-physical property of a quantum system is obtained by the scalar product:

$$\theta' = \langle A | \theta | A \rangle \quad (1.1)$$

in which A is the state of the quantum system (not an eigenstate of  $\theta$ ) and  $\theta$  is the Hermitian operator, while  $\theta'$  is the mean value of the chemical-physical property considered. Using an infinite basis set, that is the eigenstates of the position of a single particle, the average value of the observable  $\Theta$  when the microscopic system is in the state A can be written as:

$$\theta' = \sum_i \langle A | x_i \rangle \langle x_i | \theta | x_i \rangle \langle x_i | A \rangle \quad (1.2)$$

The operator associated to the total energy of the microscopic system is called Hamiltonian.

The Schrodinger equation is the eigenvalue equation defining the mean values of the Hamiltonian operator in a representation in which the auto functions are the auto states of the electron position operator. This basis equation, enunciated in 1926, is the basis of the modern quantum mechanics:

$$H\Psi(x) = E\Psi(x) \quad (1.3)$$

where  $H$  is the Hamiltonian operator and  $E$  is the energy of the system. The solutions to the equation 1.3 are the stationary auto states of the energy of the system under investigation. The solution with the lowest energy,  $E_0$ , represents the ground state. One of the fundamental assumptions made in quantum chemistry is that of Born and Oppenheimer. It assumes that since the nuclei are so much more massive and slow than the electrons they can be considered stationary while the electrons move quickly in the field of fixed nuclei. Thus, the nuclear and electronic motions are separable. This assumption has the effect of simplifying the Hamiltonian of the electronic system since the kinetic energy of the nuclei tends to be zero and the inter-nuclear repulsion term becomes a constant. The total electronic Hamiltonian can then be separated into an electronic and a nuclear component. Then, in the Born and Oppenheimer approximation, the problem is to obtain the electronic structure of an ensemble of fixed nucleus. The computational effort for the exact solution of this problem scales exponentially with respect to the number of electrons of the system. As consequence, several approximations have been developed, the simplest being the Hartree–Fock (HF) theory. According to the HF theory, in each quantum system, electron moves in a mean field generated by the other electrons and nuclei of the system. In this case, the many-electron Schrödinger equation is reduced to a mono electron problem in which each electron of the many-body system experiments the electrostatic field of nuclei and the average fields of the electrons. The HF method provides the basis for many other accurate methods.

In particular, the HF solution is the auto functions and eigenvalues that are the orbitals and their energies of the electrons forming molecules and atoms, respectively. From electronic orbitals, it is possible to obtain the electron density and the average value of each observable of the quantum system, thus also the total energy. The total energy carried out by the HF method must be considered as an approximation of the real energy of the quantum system in its ground state,  $E_0$ . The variational principle says that an approximation of the energy of a quantum system obtained from a Hamiltonian is always higher than that of the real ground state.

$$E^{approx} \geq E_0 \tag{1.4}$$

The difference between  $E_0^{HF}$  and  $E_0$  is defined as the correlation energy. Therefore, while the exchange energy between 2 electrons due to the exclusion principle of Pauli is



evaluated in the HF theory, the energy due to the interaction of contrary spin is not taken into account in this approximation.

There are several ways to evaluate the aforementioned correlation energy. The most common methods are configuration interaction (CI) and coupled cluster (CC). Both of them provide a systematic way to converge towards the exact solution. Another useful approximation is the theory of perturbations as implemented by C.Møller and M.S. Plesset (MPPT).

The Density Functional Theory assumes that the information on the system can be obtained from the electron density and thus it does not actually solve the Schrodinger equation. The DFT is not just a smart way to evaluate the correlation energy; it can be considered a new approach to the quantum mechanics.

### 1.3 Density Functional Theory

The foundation of modern DFT rests on two theorems by Hohenberg and Kohn. The first one establishes a one-to-one correspondence between the exact many-body ground-state wave function and the corresponding electron density,  $\rho(r)$ . It states: the external potential  $v(r)$  is determined, within a trivial additive constant, by the electron density  $\rho(r)$  of the considered quantum system. Since  $\rho(r)$  determines the number of electrons, it follows that  $\rho(r)$  also determines the ground-state wave function  $\Psi$  and all other electronic properties of the system. Thus, also the energy of the ground-state. This energy is, therefore a function of the electronic density and as a consequence of the external potential. For each external potential only correspond one electronic density:

$$E[\rho] = \int \rho(r) \cdot v(r) \cdot dr + F_{HK}[\rho] \quad (1.5)$$

where

$$F_{HK}[\rho] = T[\rho] + V_{ee}[\rho] \quad (1.6)$$

where which  $T[\rho]$  is the kinetic energy and  $V_{ee}[\rho]$  is the electron-electron interaction energy. The classical part of  $V_{ee}[\rho]$  is the Coulomb potential energy. To produce the separation out of the exact kinetic energy of a non-interacting system with equal number

of electrons of the considered interacting system, the FHK functional (1.6) can be rewrite as:

$$F_{\text{HK}}[\rho] = T_s[\rho] + J[\rho] + E_{xc}[\rho] \quad (1.7)$$

with

$$E_{xc}[\rho] = T[\rho] - T_s[\rho] + V_{ee}[\rho] - J[\rho] \quad (1.8)$$

Being  $T_s[\rho]$  the non-interacting kinetic energy,  $J[\rho]$  the Coulomb potential energy. The defined quantity  $E_{xc}[\rho]$  is called the “exchange-correlation energy”. It contains the difference between  $T$  and  $T_s$  kinetic energy and the non-classical part of  $V_{ee}[\rho]$ . Therefore, the exchange correlation energy” can be estimated using this functional, unlike above HF Theory.

The second theorem provides the energy variational principle. It reads: for a trial density  $\bar{\rho}(r)$ , such that  $\bar{\rho}(r) \geq 0$  and  $\int \bar{\rho}(r) \cdot dr = N$ , where  $N$  is the number of electrons of the system, the energy of the ground state is always smaller than energy obtained by the functional in which  $v$  is the aforementioned external potential:

$$E_0 \leq E_v[\bar{\rho}] \quad (1.9)$$

Assuming the differentiability of  $E_v[\bar{\rho}]$ , the variational principle requires that the ground state density satisfies the stationary principle:

$$\delta \left\{ E_v[\rho] - \mu \left[ \int \rho(r) \cdot dr - N \right] \right\} = 0 \quad (1.10)$$

which gives the Euler-Lagrange equation

$$\mu = \frac{\delta E_v(\rho)}{\delta \rho(r)} = v(r) + \frac{\delta F[\rho]}{\delta \rho(r)} \quad (1.11)$$

A useful procedure to obtain the  $\rho(\mathbf{r})$  of the ground state energy was made by Kohn and Sham. They did not resolve directly the above Euler-Lagrange equation. They defined the  $\rho(\mathbf{r})$  as function of molecular or atomic orbitals, as follows:

$$\rho(\mathbf{r}) = \sum_i^n |\psi_i(\mathbf{r})|^2 \quad (1.12)$$

Then, the total functionals (1.5) and (1.7) can be rewritten as function of these orbitals with the constrain of the orbitals orthonormality. The functional of the total energy written as function of  $\psi_i(\mathbf{r})$  has to satisfy the stationary principle (1.10):

$$\delta\Omega[\{\psi_i\}] = 0 \quad (1.13)$$

Finally, the orbitals, defining the electron density solution (1.12), are given by the Kohn and Sham equations:

$$\left( -\frac{1}{2}\nabla_i^2 + v_i^{\text{eff}} \right) \psi_i = \varepsilon_i \psi_i \quad (1.14)$$

where

$$v_i^{\text{eff}}(\mathbf{r}) = v(\mathbf{r}) + \frac{\delta J[\rho]}{\delta \rho(\mathbf{r})} + \frac{\delta E_{\text{xc}}[\rho]}{\delta \rho(\mathbf{r})} = v(\mathbf{r}) + \int \frac{\rho(\mathbf{r}')}{|\mathbf{r} - \mathbf{r}'|} \cdot d\mathbf{r} + v_{\text{xc}}(\mathbf{r}) \quad (1.15)$$

$\varepsilon_i$  are Lagrange multipliers for the orbitals orthonormality constraints. Exploiting the definition of the total energy functional given in the equation (1.7), the  $\varepsilon_i$  values can be associated to the eigenvalues of the one electronic orbitals  $\psi_i$  that is the energies of these orbitals.

## 1.4 Non covalent interactions

Atoms and molecules can interact together leading to the formation of either a new molecule (reactive channel) or a molecular cluster (nonreactive channel), respectively. In the former case, covalent interactions are clearly involved; in the latter, in which a

covalent bond is neither formed or broken, noncovalent or van der Waals (vdW) interactions are implicated. This nomenclature is, however, not well-defined and the term vdW interactions is sometimes used only for certain noncovalent interactions (mostly dispersion, see later). The noncovalent interactions were first recognized by J. D. van der Waals[8] in the last century and helped him to reformulate the equation of state for real gases. Noncovalent interactions are considerably weaker than covalent interactions. The role of noncovalent interactions in nature was fully recognized only in the last two decades; they play an important role in chemistry and physics. They are of key importance in the bio-disciplines. The structures of liquids, solvation phenomena, molecular crystals, physisorption, structures of macromolecules such as DNA and proteins, and molecular recognition are only a few examples in which noncovalent bonds are fundamental. The noncovalent interactions define the supramolecular chemistry area [9]. Non covalently assisted synthetic procedures are used to assemble various types of supramolecular species. Supramolecular chemistry offers incredible applications in various fields such as medicinal chemistry (drug delivery systems) [10-13], host-guest chemistry [14], catalysis [15-17], and molecular electronics [18]. Covalent and noncovalent interactions differ considerably and have completely different origins. A covalent bond is formed when partially occupied orbitals of interacting atoms overlap and consists of a pair of electrons shared by these atoms. Noncovalent interactions are known to act at distances of several angstroms and the overlap is thus unnecessary; in fact the overlap between occupied orbitals leads only to repulsion. The reason for the attraction between interacting subsystems must be sought elsewhere and it can lie only in the electrical properties of the subsystems. Noncovalent interactions originate from interaction between permanent multipoles, permanent multipole and induced multipole, instantaneous multipole and induced multipole and finally between instantaneous multipoles. The respective energy terms, called electrostatic, induction, and dispersion are basically attractive. However, the electrostatic term, depending on the orientation of the subsystems, can be attractive or repulsive. The repulsive term, due to the electron-electron repulsion and connected with the above mentioned overlap of occupied orbitals, prevents the subsystems approaching too closely. It is useful to consider how covalent and noncovalent interactions differ. First, there is the difference in stabilization energy and equilibrium distance: noncovalent clusters have a characteristic stabilization energy of few kilocalories per mole with intermolecular distances of about or larger than 2 Å, while covalently bound molecules have typical

binding energies of about 100 kcal/mol with typical interatomic distances below 1.5 Å. It is important to remark that the ionic bonds even being noncovalent bonds show a high binding energy as shown in Table 1.1. Entropy, always, plays a dominant role in noncovalent interactions. In fact, in the covalent interactions, the enthalpy is larger than the entropy term, and therefore, the respective change of free energy is determined mainly by the enthalpy energy term. On the contrary, in the case of the noncovalent bonds, the enthalpy terms are smaller than values related to the covalent ones therefore the entropy can assume a relevant importance. An important difference concerns the potential energy surface (PES), which is much richer of minima and maxima for noncovalent clusters. The number of energy minima of larger clusters is bigger, and to find these on a PES requires effective search method. On the basis of perturbation theory, the total stabilization energy of noncovalent complexes can be partitioned into various energy contributions. As mentioned above, the electrostatic, induction, dispersion terms and charge-transfer, form the dominant attractive contributions. The relative importance of these energy terms differ for specific types of noncovalent clusters. In some cases, one particular energy term is dominant. Typically, various attractive terms contribute to the overall stabilization of noncovalent clusters: the complexes showing hydrogen bonds provide a typical example. To describe and study noncovalent interactions, it is essential to apply the most accurate methods of quantum chemistry.

Synthetically, the types of noncovalent interactions can be summarised as follows: hydrogen bonds (H-bonds), electrostatic interactions which include both the ion-ion and also the dispersion forces, and the charge-transfer interactions. In table 1.1, these noncovalent interactions are summarized with the relative strength.

**Table 1.1:** Classification of noncovalent interactions

| Bond type           | Dependence with r   | Binding energy [kcal/mol]             | Relative strength |
|---------------------|---------------------|---------------------------------------|-------------------|
| Hydrogen bond       | -                   | 5 [25]<br>0.9-14 [26]<br>0.5-1.2 [27] | Weak-medium       |
| Ion-ion             | (1/r)               | 60 [25]<br>24-84 [26]                 | strong            |
| Dipole-dipole       | (1/r <sup>3</sup> ) | 0.5 [25]<br>1.2-12 [26]               | Weak-medium       |
| Dispersion (London) | (1/r <sup>6</sup> ) | 0.5 [25]<br><1.2 [26]                 | weak              |
| Cation – $\pi$      | -                   | 1.2-19 [26]                           | medium            |

The hydrogen bond, electrostatic and dispersion interaction will be described below because among the reported noncovalent interactions, they are supposed to be the driving forces of the increased affinity towards aminic compounds showed by the imprinted membranes described in chapter 3 of this thesis.

### 1.4.1 Hydrogen Bonding

H-bonded complexes are by far the most important and numerous noncovalent complexes [19]. The formation of a X-H...Y H-bond is accompanied by an elongation of the X-H bond which causes a decrease (red-shift) of the respective X-H stretching frequency. The red-shift is easily observable and provides unambiguous evidence about the formation of a noncovalent H-bonded complex. In general, the H-bonds have electronegative atoms as X, with Y either an electronegative atom having one or two lone pairs or a group with a region of excess of electron density (e.g.,  $\pi$ -electrons of aromatic systems). In Table 1 the classification and some properties of the hydrogen bonds are reported.

**Table 1.2:** Classification and some properties of hydrogen bonds.

| <b>D-H...A interaction</b>                   | <b>Strong</b>  | <b>Moderate</b>             | <b>Weak</b>                                |
|--|--|-----------------------------|--|
|  | <b>Mainly covalent</b>                                 | <b>Mainly electrostatic</b> | <b>Electrostatic</b>                       |
| Binding energy<br>( kcal/mol <sup>-1</sup> ) | 14–29  | 3.9–14                      | < 2.9                                      |
| Bond lengths (Å): H...A                      | 1.2–1.5  | 1.5–2.2                     | 2.2–3.2                                    |
| Bond angle ( degree )                        | 175–180  | 130–180                     | 90–150                                     |
| Examples                                     | Gas phase dimers with strong acids/bases, HF complexes | Acids, Biological molecules | C-H...N/O and N/O-H... $\pi$ hydrogen bond |

What is the driving force for geometrical and spectral evidences of H-bonding? By natural bond orbital analysis it was shown [20] that it is the charge transfer (CT) from the lone pair or  $\delta$ -molecular orbitals of the electron donor (proton acceptor) to the orbitals of the X-H bond of the electron acceptor (proton donor). An increase of the electron density in X-H orbitals causes elongation of the X-H bonds, which causes the red-shift of the X-H stretching frequency. This is accompanied by a very small CT that usually does not exceed more than 0.01 a.u. The CT is, however, considerably more important for ionic clusters. Depending of the orbitals overlapping of donator and acceptor involved in the hydrogen bond, the distance between hydrogen and acceptor varies. If that distance is between 1.2 and 1.5 Å the formed bond is mainly covalent, if is between 1.5 and 2.2 Å is mainly electrostatic and finally longer distances produce electrostatic interactions. Both C-H...Y as well as C-H... $\pi$  types of H-bonds have been observed [21,22]. If the hydrogen atom of a CH group is acidic, it can form quite strong H-bonds, otherwise, the C-H...Y hydrogen bonds are much weaker than OH...Y or NH...Y H-bonds. Nevertheless, C-H...Y H-bonds could play an important role in biomolecular structures due to their large number. The other two types of intermolecular bonds with participation of hydrogen, namely the improper (blue-shifting) H-bond and the dihydrogen bond, were described only recently, and they are less numerous than H-bonds. The C-H... $\pi$  improper (blue-shifting) H-bond was theoretically predicted in carbon proton donor...benzene complexes [23]. The manifestation of this bond is completely opposite to that of a normal H-bond, i.e., instead of an elongation of the X-H

bond and a red-shift of the X-H stretch vibrational frequency upon complex formation, there is a contraction of the bond length and a blue-shift of the stretch frequency. The dihydrogen bond such as  $M-H\cdots H-Y$  was originally found [24] in metal complexes ( $M$  = metal element) and later detected in the  $H_3BNH_3$  dimer. The explanation of this unconventional H-bond is straightforward: two hydrogens may interact weakly if one is bound to an electropositive element and the other to a very electronegative element. Consequently, one hydrogen has positive and the other has negative charge and there is a multipole attraction between these hydrogens.

### 1.4.2 Electrostatic Interactions (Dipolar Interactions)

There are various types of electrostatic interactions. The ion-dipole, ion-induced dipole, dipole-dipole, induced dipole-dipole should be taken into account. They are much weaker than ionic or covalent bonds and have a significant effect only when the molecules involved are close together (touching or almost touching).

Ion-dipole interactions are attractive force that results from the electrostatic attraction between an ion and a neutral molecule that has a dipole. They are most commonly found in solutions, especially in solutions of ionic compounds in polar liquids. A positive ion (cation) attracts the partially negative end of a neutral polar molecule or a negative ion (anion) attracts the partially positive end of a neutral polar molecule.

Dipole-dipole interactions are attractive forces. They are formed between the positive end of the dipole of one molecule and the negative pole of the dipole of another molecule. Polar molecules have local density of charge positive and negative due to the differences in electronegativity of their constituent atoms. Dipole-dipole forces have strengths that range from 1.2 kJ to 5 kJ/mol and they depend on  $r^{-3}$  where  $r$  is the dipole distance, as shown in Table 1.2. Dipole-induced dipole forces result when an ion or a dipole induces a dipole on another molecule with no dipole. An ion-induced dipole attraction is a weak attraction that results when the approach of an ion or dipolar molecule induces a dipole in a nonpolar molecule by disturbing the arrangement of electrons in the nonpolar species.

### 1.4.3 Dispersion Interactions

Dispersion interactions are less directionally specific than previous electrostatic interactions. They are determined by the instantaneous fluctuation of the electrons



Induced dipole- induced dipole. Thus, also polar molecules can also have this kind of interactions. Dispersion interactions are also called London interactions. This is, for example, the case for stacked DNA base pairs ( $\pi$ -stacking). Dispersion energy plays an important role in stabilizing clusters of bio-macromolecules, where it may be the dominant attractive term. Dispersion energy is of vital importance in stacking interactions in bio-macromolecules and may be more important than stabilization by charge-transfer. In an imprecise way, the dispersion interactions are also known as hydrophobic interactions. Hydrophobic interactions represent the tendency of non-polar groups (especially hydrocarbon groups) to associate among them in aqueous solutions. This association is accompanied by little change of enthalpy and thus the process of association of non-polar groups is governed by entropy effects, because any association of systems is always connected with a negative entropy change.

## References.

- [1] Jensen, F., *Introduction to Computational Chemistry* (Second Edition) , John Willey & Sons Ltd (2007).
- [2] Clark, T., *A Handbook of Computational Chemistry*, Wiley, (1985).
- [3] Levine, I. N., *Quantum Chemistry*. Fifth ed.; Prentice Hall, Inc, (2000).
- [4] Szabo, A., Ostlund, N. S., *Modern Quantum Chemistry: Introduction to Advanced Electronic Structure Theory*. McGraw-Hill, Inc, (1989).
- [5] Koch, W., Holthausen, M.C., *A Chemist's Guide to Density Functional Theory*. Second ed.; Wiley-VCH, (2001).
- [6] Bader, R. F. W., *Atoms in Molecules: A Quantum Theory*. Oxford University Press, (1990).
- [7] Popelier, P., *Atoms in Molecules: An Introduction*. Pearson Education Limited, (2000).
- [8] Van der Waals, J. D., *Doctoral Dissertation*, Leiden, (1873).
- [9] Lehn, J.M., Atwood, J. L., Davies, J. E. D., MacNicol, D. D., Vögtle, F., *Comprehensive Supramolecular Chemistry* Eds.; Pergamon: Oxford, (1996).
- [10] Duncan, R.; Kopecek, J., *Adv. Polym. Sci.* (1984), 57, 51.
- [11] Peppas, N. A.; Nagai, T., Miyajima, M., *Pharm. Technol. Jpn.* (1994) 10, 611.
- [12] Bieniarz, C., *Technology Encyclopedia of Pharmaceutical*; Marcel Dekker: New York, (1999), p 55.
- [13] Akiyoshi, K., *Kagaku (Kyoto)* (1994) 49, 442.
- [14] Tzalis, D.; Tor, Y. *Tetrahedron Lett.* (1996) 37, 8293.
- [15] Huck, W. T. S.; Prins, L. J.; Fokkens, R. H.; Nibbering, N. M.; van Veggel, F. C. J. M.; Reinhoudt, D. N., *J. Am. Chem. Soc.* (1998) 120, 6240.
- [16] Knapen, J. W. J., van der Made, A. W., de Wilde, J. C., van Leeuwen, P. W. W. N. M.; Wijkens, P., Grove, D. M.; van Koten, G., *Nature* (1994) 372, 659.
- [17] Kokufuta, E., *Adv. Polym. Sci.* (1993) 110, 157.
- [18] Warshel, A., Papazyan, A., Kollman, P. A., *Science* (1995) 269, 102.
- [19] Scheiner, S., *Hydrogen Bonding. A Theoretical Perspective*; Oxford University Press: New York, (1997).
- [20] Starikov, E. B., Steiner, T., *Acta Crystallogr., Sect. D* (1997) 53, 345.
- [21] Steiner, T., Desiraju, G. R., *Chem. Commun.* (1998), 891.

- [22] Djafari, S., Barth, H.D., Buchold, K., Brutschy, B., *J. Chem. Phys.* (1997) 107, 10573.
- [23] Reed, A., Curtiss, L. A., Weinhold, F., *Chem. Rev.* (1988) 88, 899.
- [24] Lee, J. C., Peris, E., Rheingold, A. L., Crabtree, R. H., *J. Am. Chem. Soc.* (1994) 116, 11014.
- [25] Atkins, P. W., *Physical chemistry*. VCH: Weinheim, (1996).
- [26] Steed, J. W., Atwood, J. L., *Supramolecular chemistry*; John Wiley & Sons(2000).
- [27] Perrin, C. L., Nielson, J. B., *Annu. Rev. Phys. Chem.* (1997) 48, 511.

# **Chapter 2**

## **Molecular imprinting Technique and Membrane Technology**

## **2.1 The Molecular Imprinting Technique**

During the last decades the utilization of molecularly imprinted polymers (MIPs) in many research areas has been extensively developed. The result of this development, has been a spectacular and progressive increasing of the related works published per year. Two main approaches for molecular imprinting were proposed. In the procedure firstly proposed by Wulff [1] and called covalent molecular imprinting, the complex functional monomer-template interacts by a covalent bond and is later polymerized. The second approach was proposed by Moshbach [2] and named non-covalent imprinting. In this way a cross-linked polymer interacted with the template molecule simply through electrostatic interaction, hydrogen bonding or similar non-covalent bonds. Recently, the semi-covalent approach has been also described [3-4]. This method combines both procedures previously described. Utilization of molecular imprinting technique has been widely reported for the preparation of molecularly imprinted polymers (MIPs). Actually, MIPs technology is strong and robust tool widely studied and developed. It has a large established market and is extensively utilised in a great variety of different applications. For instance, MIPs have been used as sensors for detection of various compounds,[5,6] in recognition studies [7,8], chiral separations [9,10], mimicking of binding sites of antibodies, receptors,[11] and enzyme catalysis [12]. Membrane technology had started to be used and developed a long time before the born of imprinting technique and was a consolidated and potent tool in the ambit of molecular separations. The challenge of involve MIPs in the membrane preparation process suddenly attracted the attention of numerous scientists because opened a new innovative way in molecular separations and represented a strong and cheap alternative to chromatographic methods. The first work involving molecularly imprinted membranes (MIMs) was proposed, as mentioned in the preface, at the beginning of the 90s. An exhaustive discussion about membrane technology including MIMs technology is exposed bellow.

## **2.2 Membrane Technology**

A membrane is an inter phase between two adjacent phases acting as a selective barrier, regulating the transport of substances between the two compartments[13]. The main advantages of membrane technology as compared with other unit operations in chemical engineering are related to the transport selectivity of the membrane. Separations processes with membranes do not require additives, and they can be performed

isothermally at low temperatures and compared with other thermal separation processes- at low energy consumption. Membranes have gained an important place in chemical technology and are used in a broad range of applications[13,14]. The key property that is exploited is the ability of a membrane to control the permeation rate of a chemical specie through the membrane.

In controlled drug delivery, the goal is to moderate the permeation rate of a drug from a reservoir to the body. In separation applications, the goal is to allow one component of a mixture to permeate the membrane freely, while hindering permeation of other components.

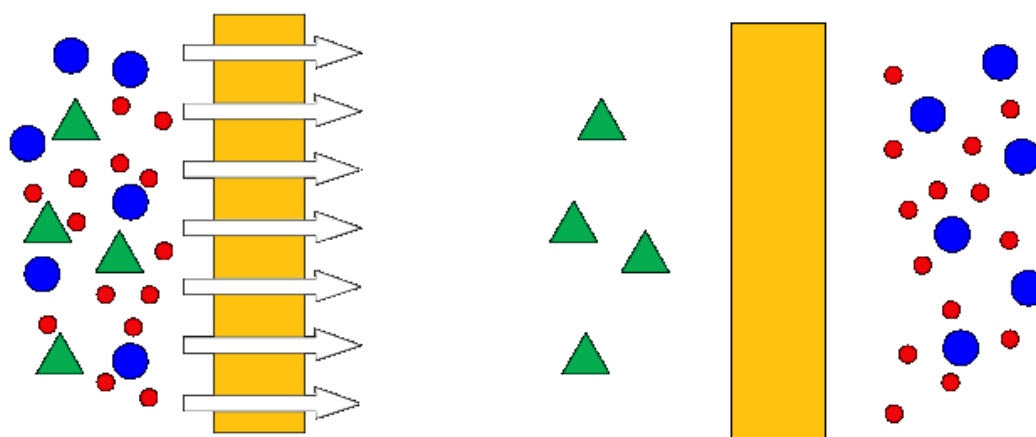


**Figure 2.1:** Illustration of a membrane used in molecular separations.

The major examples are water purification by reverse osmosis and blood detoxification by dialysis or ultrafiltration. Membranes have also big importance in the food and pharmaceutical industry as well as the process and waste water treatment. Other important applications have been realized in gas separation. Today synthetic separation membrane processes can be classified according different criteria:

\*Membrane materials: Organic polymers, inorganic materials (oxides, ceramics, metals...) organic-inorganic compositated materials.

\*Preparation Method: Phase inversion of polymer solution, sol-gel process towards inorganic or organic-inorganic materials, interface reaction towards thin-layer composite, stretching, extrusion, track-etching, micro-fabrication.

\*Membrane shape: Flat-sheet, hollow fibre, hollow capsule.

During this PhD I worked with flat-sheet and composite MIMs (Molecular Imprinted Membranes) synthetic membranes made of organic polymers and prepared by Phase inversion Technique for the removal of some impurities in non aqueous systems.

### **2.2.1 Background**

Systematic studies of membrane phenomena can be traced to the eighteenth century philosopher scientists. For example, Abbe Nolet coined the word ‘osmosis’ to describe permeation of water through a diaphragm in 1748. Through the nineteenth and early twentieth centuries, membranes had no industrial or commercial uses, but were used as laboratory tools to develop physical/chemical theories. For example, the measurements of solution osmotic pressure made with membranes by Traube and Pfeffer were used by Vant Hoff in 1887 to develop his limit law, which explains the behaviour of ideal dilute solutions; this work led directly to the Vant Hoff equation. At about the same time, the concept of a perfectly selective semi permeable membrane was used by Maxwell and others in developing the kinetic theory of gases. In 1907, Bechhold devised a technique to prepare nitrocellulose membranes of graded pore size, which he determined by a bubble test [15]. Other early workers, particularly Elford [16], Zsigmondy and Bachmann [17] and Ferry [18] improved on Bechhold’s technique, and by the early 1930s, microporous colloidal membranes were commercially available. During the next 20 years, this early microfiltration membrane technology was expanded to other polymers, notably cellulose acetate. Membranes found their first significant application in the testing of drinking water at the end of World War II. Drinking water supplies serving large communities in Germany and elsewhere in Europe had broken down, and filters to test for water safety were needed urgently. The research effort to develop these filters, sponsored by the US Army, was later exploited by the Millipore Corporation, the first and still the largest US microfiltration membrane producer.

By 1960, the elements of modern membrane science had been developed, but membranes were used in only a few laboratory and small, specialized industrial applications. Membranes suffered from four problems that prohibited their widespread use as a separation process: They were too unreliable, too slow, too unselective, and too expensive. Solutions to each of these problems have been developed during the last 50 years, and membrane-based separation processes are now commonplace.

The seminal discovery that transformed membrane separation from a laboratory to an industrial process was the development, in the early 1960s, of the Loeb–Sourirajan process for making defect-free, high-flux, anisotropic reverse osmosis membranes [19]. These membranes consist of an ultrathin, selective surface film on a much thicker but much more permeable microporous support, which provides the mechanical strength. The flux of the first Loeb–Sourirajan reverse osmosis membrane was 10 times higher than that of any membrane then available and made reverse osmosis a potentially practical method of desalting water. The work of Loeb and Sourirajan, and the timely infusion of large sums of research and development dollars from the US Department of Interior, Office of Saline Water (OSW), resulted in the commercialization of reverse osmosis and was a major factor in the development of ultrafiltration and microfiltration. The development of electrodialysis was also aided by OSW funding.

Concurrently with the development of these industrial applications of membranes was the independent development of membranes for medical separation processes, in particular, the artificial kidney. W.J. Kolf had demonstrated the first successful artificial kidney in The Netherlands in 1945. It took almost 20 years to refine the technology for use on a large scale, but these developments were complete by the early 1960s. Since then, the use of membranes in artificial organs has become a major life-saving procedure. Various million people around the world are now sustained by artificial kidneys and a further million people undergo open-heart surgery each year, a procedure made possible by development of the membrane blood oxygenator. The sales of these devices comfortably exceed the total industrial membrane separation market. Another important medical application of membranes is for controlled drug delivery systems. A key figure in this area was Alex Zaffaroni, who founded Alza, a company dedicated to developing these products in 1966. The membrane techniques developed by Alza and its competitors are today widely used in the pharmaceutical industry to improve the efficiency and safety of drug delivery.

The period from 1960 to 1980 produced a significant change in the status of membrane technology. Building on the original Loeb–Sourirajan technique, other membrane formation processes, including interfacial polymerization and multilayer composite casting and coating, were developed for making high performance membranes. Using these processes, membranes with selective layers as thin as 0.1  $\mu\text{m}$  or less are now being produced by a number of companies. Methods of packaging membranes into large-membrane-area spiral-wound, hollow-fine-fiber, capillary, and plate-and-frame



modules were also developed, and advances were made in improving membrane stability. By 1980, microfiltration, ultrafiltration, reverse osmosis and electro dialysis were all established processes with large plants installed worldwide.

The principal development in the 1980s was the emergence of industrial membrane gas separation processes. The first major development was the Monsanto Prism membrane for hydrogen separation, introduced in 1980. Within a few years, Dow was producing systems to separate nitrogen from air, and Cynara and Separex were producing systems to separate carbon dioxide from natural gas. The final development of the 1980s was the introduction by GFT, a small German engineering company, of the first commercial pervaporation systems for dehydration of alcohol. Membrane gas separation technology has been extensively investigated and developed in the last 3 decades. In one world already conscious with global warming and with the necessity to preserve the natural resources, the main object of study has been the carbon dioxide separation and capture. During the decade of 1990s appeared the so-know as molecularly imprinted membranes. There is a section in this chapter exclusively dedicated to this particular kind of membranes.

## **2.2.2 Recent trends concerning the membrane technology**

Today membrane technology is widely studied, applied and developed. Membranes and membranes based devices are present in our daily life and they make it easier. I will explain briefly the breakthroughs and recent novelties produced during the last years concerning the most important areas of membrane technology.

Nowadays, the hottest highlights in membrane technology concern about water treatment, chemical/biomedical applications, gas separations, and environmental applications. It is important to emphasize that membrane technology has an enormous number of other applications that will not be mentioned here. This is just a small resume of the applications about 4 big important and essential areas inside the wonderful world of membranes.

### **2.2.2.1 Membranes for water treatment**

The main goal regarding the water treatment is the production of ultra pure water from different sources. Because of vastly expanding populations, increasing water demand, and the deterioration of water resource quality and quantity, water is going to be the

most precious resource in the world. Thus, the 21st century is called the “water century.” In the 20th century, membrane technologies made great progress, and commercial markets have been spreading very rapidly and throughout the world. Since largest source of water is the sea numerous works have been addressed to obtain ultra pure water from sea water by the process known as seawater desalination. Seawater desalination is the production of fresh, low-salinity potable or industrial-quality water from a saline water source (sea, bay, or ocean water) *via* membrane separation or evaporation. Today, seawater desalination is mostly used to produce fresh potable water for human consumption and crop irrigation. Industrial applications of desalinated seawater are typically limited to its use as a low-salinity power plant boiler water, process water for oil refineries, chemical manufacturing plants, and commercial fishing installations, canneries and other food industries. The limited industrial use of seawater desalination is related mainly to the high costs associated with production of high-purity or ultrapure water from seawater. Most industrial water supply facilities use low-cost groundwater or brackish water to produce high industrial-grade water for their specific applications.

Approximately 97.5% of the water on our planet is located in the oceans. Therefore, it is classified as seawater. Of the 2.5% of the planet’s freshwater, approximately 70% is in the form of polar ice and snow; and 30% is groundwater, river and lake water, and air moisture. So even though the volume of Earth’s water is vast, less than 10 million of the 1400 million m<sup>3</sup> of water on the planet are of low salinity and are suitable for use after applying conventional water treatment only. Seawater desalination provides means for tapping the world’s main water resource—the ocean. The mineral/salt content of the water is usually measured by the water quality parameter total dissolved solids (TDS), in milligrams per liter (mg/L) or parts per thousand (ppt).

Natural water sources such as sea, bay, and ocean waters usually have TDS concentration higher than 15000 mg/L. Seawater TDS and temperature are the two key source water quality parameters that have the most significant influence on the cost of seawater desalination. Source water quality has a key influence on the suitability of using seawater desalination for industrial water supply. The water quality parameters that have a significant impact on the desalination system design, operations, and cost of water production are the concentration of TDS, chlorides, turbidity, silt density index (SDI), organic content, nutrients, algae, bacteria, temperature, boron, silica, barium, calcium, and magnesium.

Desalinated water quality is driven by its use. Typically, potable use of desalinated seawater is closely related to the levels of TDS, chlorides, boron, and bromides in this water. Drinking water regulations worldwide usually establish levels of TDS and chlorides in the product water below 500 and 250 mg/L, respectively. However, when using desalinated seawater, the importance of these parameters is often overshadowed by the health and irrigation-related water quality requirements in terms of boron and disinfection-related water quality targets in terms of bromides. The main reason boron and bromides are of specific importance for the overall quality of the desalinated water is the fact that their concentration in seawater is usually an order of magnitude higher than that of typical freshwater sources (rivers, lakes, groundwater, etc.). For example, typical river water has boron concentration of 0.05–0.2 mg/L, while the seawater boron levels are usually between 4.0 and 6.0 mg/L. Similarly, the bromide levels in freshwater sources are usually between 0.05 and 0.3 mg/L, while seawater has bromide concentration of 55–85 mg/L. While RO membranes typically remove over 70% of the boron and over 99% of the bromides in the source seawater, the remaining levels of these compounds are still several times higher than that in fresh surface water sources. Usually, the boron level in the desalinated water is required to be less than 0.5 mg/L in order to alleviate problems associated with the use of this water for irrigation of sensitive crops (e.g., citrus trees, avocados, strawberries) or ornamental plants. To achieve this level of boron in the desalinated water, often the water TDS and chloride levels have to be reduced below 100 and 50 mg/L, respectively. The bromide concentration of the desalinated seawater may also have a significant effect on the required level of removal of salts from the seawater, especially if this water will be disinfected using chloramines rather than chlorine, or it will be ozonated. While using chlorine only creates a stable chlorine residual that shows minimum decay over time, applying a combination of chlorine and ammonia to create chloramines (a practice widely used in the United States for example) to desalinated water with bromide levels above 0.4 mg/L, usually yields unstable chlorine residual that decays rapidly (within several hours) to unacceptably low levels. Although the effect of high levels of bromide in the desalinated water can be mitigated by superchlorination (i.e., applying initial chlorine at dosages of 4.0 mg/L or higher), this effect has to be accounted for especially when blending this water with other water sources that have low levels of bromides. If desalinated seawater that contains bromide of levels above 0.2 mg/L is disinfected by ozonation, the ozonated water contains unacceptably high levels of bromate and is

typically above the threshold of 10 mg/L, considered suitable for human consumption. Another important drawback of ozonating desalinated water is the significant increase in the levels of brominated disinfection by-products (DBPs). Although currently individual brominated DBPs are not regulated, that is likely to occur in the near future. As a result, the target overall water quality of the desalinated seawater in some industrial applications, such as the production of bottled water where ozonation is widely practiced, may be driven by the level of bromides in the water. In addition to the potable uses discussed above, the desalinated water quality may be driven to even higher levels by the need of some industrial applications, especially those where ultrapure water quality is necessary.

Among desalination technologies available today, reverse osmosis (RO) is regarded as the most economical desalination process. Therefore, RO membranes have played crucial roles in obtaining fresh water from nonconventional water resources such as seawater and waste water. The process of desalinating sea water with membranes of reverse osmosis is known as Seawater reverse osmosis desalination (SWRO) desalination. Reverse osmosis membranes have been used widely for water treatment such as ultrapure water makeup, pure boiler water makeup in industrial fields, seawater and brackish water desalination in drinking water production, and wastewater treatment and reuse in industrial, agricultural, and indirect drinking water production. The expansion of RO membrane applications promoted the redesign of suitable membrane material to take into consideration chemical structure, membranes configuration, chemical stability, and ease of fabrication. And along with the improvements of the membranes, the applications are further developed [20]. It is very important to increase the water recovery ratio on seawater desalination systems to achieve further cost reduction. Most seawater RO desalination systems in use today are confined to approximately 40% conversion of the feed water (salt concentration 3.5%), since most of commercially available RO membrane do not allow for high-pressure operation of more than around 7.0MPa.

Recent progress on high-pressure–high-rejection spiral wound (SW) RO elements, combined with proven and innovative energy recovery and pumping devices, has opened new possibilities to reduce investment and operating cost. Toray has developed a new low-cost seawater desalination system called the Brine Conversion Two-Stage (BCS) system, which provides 60% water recovery of freshwater (Yamamura et al., [21] and Ohya et al. [22] also suggest that higher recovery of RO seawater desalination

by the BCS system is most effective in saving energy yet keeping a low operating cost. As for achieving the 60% RO seawater desalination system, it is absolutely necessary to make the RO membrane element, which can be operated under very severe operating conditions, with high pressure and high feed water concentration. Toray has developed a high-performance membrane (BCM element) that can be operated at high pressure and high concentration conditions.

The removal of boron is a significant problem in SWRO desalination processes [23]. Boron exists as boric acid in the natural water, and boric acid mainly shows the male reproductive tract when administered orally to laboratory animals. The World Health Organization (WHO) proposes that boron concentration in drinking water be below 0.5mg/ L as a provisional guideline value [24]. However, especially in SWRO desalination fields, this is not an easy goal to meet because boron concentration in seawater is comparatively high. Although conventional SWRO membrane elements have shown a little more than 90% of boron rejection, it is still inadequate. It is difficult for RO membranes to remove boric acid in water for the following reasons: First, the molecular size of boric acid is so small that it is difficult to remove by size exclusion. Second, since boric acid has a pKa of 9.14–9.25, it is not ionized in natural seawater with a pH of 7.0–8.0 and dissociates at pH 9 or more [25]. The boron rejection by the electric repulsive force between boric acid and the membrane cannot be expected in a neutral condition. Therefore, some post treatment processes are necessary to meet the WHO proposal. The conventional SWRO membrane element TM820, which is typical with Toray, has exhibited 91–93% boron rejection, which was the highest level achieved by commercialized SWRO membrane elements [26–28]. This membrane element series has been installed in a large number of SWRO. plants. And Toray® has commercialized many types of SWRO membrane elements, which are for different pressure ranges due to total dissolved solids (TDS) concentration and temperature of the seawater. However, the highest boron rejection in those membrane elements is 91–93%, which is the same as TM820. This means that the improvement of boron rejection by membrane material had been sluggish for a while. Meanwhile, the new membrane element TM820A was developed based on the following two concepts:

(1) reduction of affinity with boric acid by control of hydrophobic property and functional groups may reject boric acid selectively, and (2) molecular structure design was considered as blocking the boric-acid-permeable large pore [29]. TM820A exhibited 94–96% boron rejection with high TDS rejection and high water productivity.

Seen from various viewpoints, a single SWRO system is the most ideal. Therefore, to evaluate the performance of TM820A, the amount of boron that TM820A could remove by a single-stage operation was estimated. TM820A meets the Japanese guidelines of below 1mg/L of boron concentration by a single-stage operation. But in severe conditions, for the WHO guideline grade and the Middle East seawater treatment, certain posttreatment processes are still needed. If 97% of boron rejection performance is gained, the WHO grade will be enabled until the Southeast Asia seawater treatment. Furthermore, at 99% boron rejection performance, the WHO guideline grade will be enabled even in the Middle East seawater treatment. Recently, Toray has been investigating SWRO membranes that focus on the removal of boron by the improvement of membrane performance although the boron rejection was also improved as various membranes were developed in each company, it was 90% at best. In the period, from 2000 to 2003, the membranes in which a little more than 90% of boron rejection was shown were released, and these serve as main items for each company now.

From 2003 to 2005, Toray developed and released TM820A, whose performance was appreciably improved, and offered the membrane that showed around 95% boron rejection prior to other companies. However, the supportive systems are still required to meet the WHO proposal even by using TM820A as above. Thus, the next target is 97 or 99% boron rejection performance of renovative membrane. The further development of a new renovative membrane that can meet the WHO proposal for every seawater continues.

Toyobo recently developed a new type of RO module made of cellulose triacetate (CTA) to achieve higher product water recovery in order to further reduce the cost of RO desalination. Toyobo's hollow-fiber RO modules are widely used around the world in RO desalination plants. Based on the long operating experience and recent research efforts, Toyobo developed the high-pressure high-flux HB series modules. The HB series is an improved version of the conventional HM series type of module using the same materials. The hollow-fiber membrane in the HB series module is wound in a cross arrangement, designed to minimize pressure loss and allow uniform water flow in the module. The hollow fiber incorporated in the HB series has higher pressure resistance based on a change of the hollow-fiber outer diameter/inner diameter dimensions and optimization of manufacturing conditions. The product flow rate of the new type improved by about 1.4 times compared with the conventional type. A high-

pressure, single-pass desalination process of new HB series modules with high recovery was successfully conducted for the first time at an RO test plant on the Red Sea at the conditions of more than 52% recovery. Toyobo developed also an advanced, large-sized new-style membrane module. This new type advanced larger sized RO module has the same basic structure of the above-mentioned and has a length about 1.5 times. The amount of product water of one module has the capability of more than 2 times (i.e., double) or a 100-m<sup>3</sup>/day capacity. The membrane material is the same CTA with the same characteristics of a cross-winding arrangement of the hollow fiber, the same excellent chlorine resistance, and stable operations are maintained. In addition to the excellent basic characteristics of CTA membranes that other membranes also offer, CTA offers a very practical characteristic that makes it useful as a RO membrane. The CTA membrane is the only RO membrane among many RO membranes currently marketed that offers this high degree of chlorine resistance. Moreover, the material of CTA in hollow-fiber form is excellent in a general fouling proof nature and has the characteristic of being difficult to become dirty with fouling matters. Furthermore, CTA in the form of a hollow-fiber membrane element in a module has a membrane area as large as about 10 times per unit volume compared with a spiral wound membrane element and significantly reduces the flux per unit membrane area. Therefore, with CTA it becomes possible to decrease membrane load, and that makes it more difficult for fouling to occur. These key attributes lead to minimum chemical cleaning and long membrane life.

#### **2.2.2.2 Membranes for chemical/biomedical applications**

Most important topics of this area of membrane technology are tissue engineering, membrane therapeutic devices for drug release, and hemodialysis. Tissue engineering belongs to an area the regenerative medicine. Regenerative medicine uses its unique approach to regenerate cells, tissues, and even organs to prevent and cure diseases and to repair, restore, and enhance functions of damaged and diseased tissues and organs. Common approaches in regenerative medicine include stem cell transplantation, cell therapy, gene therapy and tissue engineering, and their combinations, with tissue engineering and stem cell transplantation being the newest and most exciting approaches. Tissue engineering, as an identified field, was established in the late 1980s, although it has to be pointed out that such an approach may have been practiced clinically for centuries. Its basic concept is to produce live and functional tissue by

culturing appropriate cells on a three-dimensional scaffold for a certain period of time and then to implant the engineered tissue into the body to replace or repair the damaged or lost tissue. The concept has been proved and engineered skin products are available commercially. Stem cells offer unprecedented opportunities and potentials for regenerative medicine. Bone marrow transplantation is an established clinical procedure, and the transplant of blood stem cells separated from umbilical cord blood, has also been established. It is, however, the potential of using embryonic and adult stem cells to regenerate all the tissues and organs in the body that has attracted attention and imagination all over the world. If stem cell potentials materialize, or even a fraction of their potentials are materialized, the health care industry will be revolutionized. The ethical and social issues surrounding stem cell research and applications are well known—for example, where the stem cells are from and who will pay for the treatment. It must also be emphasized that stem cell research and application is still in “embryo” stage. There are many huge obstacles to be overcome before clinical application becomes a reality. The research and development in tissue engineering and stem cell therapy need an integrated effort by multidisciplinary teams. Clinical relevance and technology development play equally important roles. Due to its enormous impact, both economically and socially, huge R&D efforts have been poured into this emerging and exciting field. In 2001, the total R&D spending was about \$580 million, and the estimated market was \$15 billion just for connective structural tissues and \$10 billion for soft tissue repair worldwide (RMD report) [30].

The term membrane can have a wide range of meanings, and hence it is necessary and important to clarify at the beginning that the discussion is only limited to microporous membranes, and further the pores having the function of transmembrane transport. Application of membrane-like porous structures for engineering of thin layered tissues including skin [31], bladder [32], and cornea are excluded from the discussion.

Efficient stem cell expansion is a key bottleneck for clinical application and commercialization of stem cell therapy. Membrane bioreactors may make a significant contribution due to its important features such as possibility for uniform chemical and biochemical conditions within the bioreactor, low or even zero hydrodynamic shears, large surface-to-volume ratios, and physical separation between two cell types but allowing biochemical signaling between them. For example, it may be possible to culture the feeder cells on one side of the membrane, while culturing human embryonic stem cells on the other. In this way human embryonic stem cells are not mixed with the



feeder cells, which eliminates the need for later difficult separation, but get the biochemical signals from the feeder cells that are necessary to proliferate embryonic stem cells [33].

Membranes have been successfully applied to hemodialysis and artificial lung [34,35]. Bioartificial organs are the next generation of devices involving the use of living cells, and membranes could be an essential part of these developments[36]. Membrane devices incorporating kidney and lung cells are being studied [37], but the most studied device is probably the liver support systems [38,39]. In such devices, the advantages of offering large surface area to support cell growth of compact membrane device and providing a physical barrier to retain and confine cells are exploited. It has become obvious that new types of membranes need to be developed for tissue engineering applications. For example, some applications will require the controllable and tunable biodegradation rate, so the degradation of the membrane and scaffold can match the neotissue formation and angiogenesis [40]. Ellis and Chaudhuri [41] developed poly(lactide) (PLA) and poly(lactide-co-glycolide) (PLGA) copolymer hollow-fiber membranes and cultured osteoblasts on these hollow fibers. Some applications may need controlled mass transfer rate. Some applications may require a narrow pore size distribution, as it has been shown that pore size does affect cell adhesion and proliferation. One thing is common for all these applications: the surface properties are likely to be the most important parameter, and also these membranes are likely to be operated under ultra-low-permeate flux. For most tissue engineering applications, suitable membranes are to be developed, which provides a great opportunity for membrane research and development. The new membranes are likely to be sold by functions, instead of quantity, and with very high added values. Membrane technologies have been applied into tissue engineering or more generally regenerative medicine. As an enabling technology, application of membranes can help to overcome some key bottlenecks in tissue engineering and stem cell therapy. Other important applications, such as membrane bioreactors for stem cell expansion, immunoisolation, mass transport control, and bioartificial organs, are also briefly discussed. However, the membranes currently commercially available cannot fulfill the requirements for tissue engineering applications and hence development of new membranes with novel functions such as biodegradability, bio compatibility, and controlled release of active agents provides a good opportunity for membrane research. A new set of rules and parameters need to be defined to assess these new membranes as well. The biopharmaceutical industry is a

major user of membrane-based techniques, the main areas of application being biopharmaceutical purification, sterile filtration of pharmaceutical products and intermediates, endotoxin removal, water purification, and membrane-based biological analysis. The membrane-based technologies that are widely used are microfiltration, ultrafiltration, reverse osmosis, and membrane chromatography. The first ultrafiltration membranes ever used were developed for processing proteins. However, for a long time the use of membrane-based technologies was largely restricted to food processing, water purification, and environmental applications. Sterile filtration using microfiltration membranes was perhaps the only major biopharmaceutical application for quite a while. The widespread use of membranes in the biopharmaceutical industry did not really happen until recently. Membranes are now increasingly being used for a range of different applications. Membranes specifically designed for biopharmaceutical applications are now widely available, and we are likely to see a huge expansion in the use of membrane-based technologies in this sector. The main focus in the biopharmaceutical industry in recent years has been in the area of protein-based therapeutics. Biopharmaceutical proteins such as monoclonal antibodies, plasma proteins, interleukins, interferon, growth factors, vaccines, and hyperimmune antibodies are increasingly being purified using microfiltration, ultrafiltration, and membrane chromatography [42]. These techniques are generally less expensive, more reproducible, and more easily scalable than conventional purification techniques [43]. These are also more desirable from a process validation point of view on account of the availability of relatively inexpensive disposable membrane products [44]. Sterility is an important requirement in biopharmaceuticals, and by using membrane-based techniques, which are mostly based on barrier permeation, this attribute can be built into a purification process at multiple stages. Ultrafiltration is traditionally used for selectively removing low-molecular-weight substances such as salts, peptide fragments, and impurities from protein solutions as well as for concentrating these solutions, that is, removing water from them. Research done in the past decade has clearly demonstrated that protein-protein fractionation using ultrafiltration is feasible [45-47]. With the advent of new and improved membranes as well as new ways of carrying out ultrafiltration, this technique can easily compete with other high-resolution protein purification techniques [48]. For a long time sterile filtration mainly relied on microfiltration since this technique worked very well for efficient removal of bacterial and fungal contaminants. With virus removal from pharmaceutical products becoming mandatory, ultrafiltration is increasingly being

used for sterile filtration since these membranes are better at retaining virus particles than microfiltration membranes [49]. Ultrafiltration can also potentially capture infective prion proteins [50]. Endotoxins, which are contaminants from bacteria sources, are traditionally removed from pharmaceutical products by packed-bed adsorption. Membrane adsorption, which involves the use of membrane stacks as adsorbent, is now increasingly being used for this application on account of several vital advantages over packed bed adsorption.

Membranes are increasingly being used in the biopharmaceutical industry for a range of different applications. The main focus in the biopharmaceutical industry in recent years has been on the development and manufacture of protein-based therapeutic products. Therapeutic proteins such as monoclonal antibodies, plasma proteins, interleukins, interferon, growth factors, vaccines, and hyperimmune antibodies are processed using membrane-based techniques such as microfiltration, ultrafiltration, and membrane chromatography. Ultrafiltration is primarily used for protein concentration, desalting, and clarification. In recent years there has been a significant amount of research work done on the use of ultra filtration for protein fractionation, the overwhelming conclusion being that ultra filtration can indeed be used for protein–protein separation. However, this would be possible only under highly optimized conditions. A huge range of commercial ultra filtration membranes specifically developed for biopharmaceutical applications is now available. Configurations currently used in the industry are suitable for carrying out concentration, desalting, and clarification, but these are not suitable for fractionation. Several new configurations suitable for protein fractionation have been proposed in recent years. Also, techniques for rapidly optimizing fractionation processes are now available.

Artificial membranes are used in biomedicine to treat blood for a broad variety of therapeutic purposes. In most treatments, blood is continuously withdrawn from the patient's blood circulation and brought in extracorporeal circulation into direct contact with the artificial membranes assembled in the device where solutes are perm selectively removed from or supplied to it. The treated blood is then given back to the patient. Treatment sessions generally last a few hours and may have to be repeated a few times a week, sometimes for years. In Japan, more than 5000 uremic patients have been reported to be on hemodialysis for longer than 25 years. In these treatments, membranes are used as permselective barriers to permit transport of selected solutes to/from the blood, while hindering the loss of essential blood constituents,

and to regulate the rate at which solutes are transferred across the membrane so as to maintain the patient's homeostasis. For instance, waste metabolites are removed from renal failure patients by hemodialysis; excess water is removed from fluid overload patients by hemofiltration; plasma is separated from the blood cells of patients with immune-mediated diseases and removed by therapeutic apheresis; gaseous O<sub>2</sub> and CO<sub>2</sub> are supplied to and removed from the blood, respectively, in gas exchangers (often termed artificial lungs). A number of factors contribute to making the development of adequate membranes and devices for such processes rather complex, among which are the broad spectrum of molecular weights and physical-chemical properties of the species to be transported or rejected, the interactions between membranes and body fluids that continuously modify both membrane and blood properties, and the need for materials and processes that cause neither short-term nor long-term harm to the patient. It should also be recalled that membrane capacity to meet the set therapeutic objective, in terms of the solutes transported and the actual rate at which they cross the membrane, is determined by the intrinsic mass transport properties of the membrane, but also by the conditions under which solutes and cells are transported from the bulk of the membrane-contacting fluids to the membrane surface.

### **2.2.2.3 Membranes for gas separation.**

The two principal suppliers of vapor-gas membrane separation systems are MTR and the licensees of GKSS (Borsig, Sihi, and Dalian Eurofilm). The major markets serviced by these companies are described briefly below.

Probably the largest single application of vapor separation membranes is in the recovery of hydrocarbon monomers from ethylene and polyethylene and polypropylene plants. These plants make polyolefins, principally from ethylene and propylene. After the polyolefin resin is produced, it contains unreacted monomer and hydrocarbon solvents, dissolved in the resin powder. The dissolved hydrocarbon must be removed before the polymer can be used, and this is done by stripping with hot nitrogen in a column known as a degassing bin. In early polyolefin plants, the vent gas from the degassing bin—containing 10–20 mol% hydrocarbon—was used as boiler fuel. Since the development of vapor separation membranes, most new polyolefin plants have installed hydrocarbon recovery units. In a modern polyolefin plant, the value of the monomer in the nitrogen resin bin off-gas is on the order of \$1–2 million/year; the value of the nitrogen can represent another \$0.5 million/year. Recovery and reuse of these components is well

worthwhile. A process flow stream and a photograph of a typical membrane system fitted to a polyolefin plant resin degassing bin was proposed by 60 Baker and Jacobs, 1996. A portion of the propylene then condenses. The condenser overhead stream (propylene and nitrogen) is sent to the membrane section, which contains two membrane units in series. The first membrane unit produces a permeate stream enriched in propylene and a purified residue stream containing 97–98% nitrogen. The vapor-enriched permeate stream is recycled to the inlet of the compressor. The nitrogen-rich residue can often be directly recycled to the degassing bin without further treatment. However, in the example shown, the residue gas is passed to a second membrane unit to upgrade the nitrogen to better than 99% purity. The waste hydrocarbon stream from the second membrane unit is sent to flare. During the last 10 years, almost 50 of these systems have been installed around the world.

Another basic important application of membrane vapor recovery systems is the recovery of gasoline vapors from vent streams produced at large oil and gasoline terminals. During the transfer of hydrocarbons from tankers to holding tanks and then to trucks, off-gases are produced. The off-gas stream volume and vapor concentration vary widely, but the average emissions resulting from each transfer operation are large—in the range of 0.03–0.05% of the hydrocarbon transferred [51,52]. The hydrocarbon concentration of the emitted gas is generally quite high, in the range of 10–30 vol%, depending on the type of hydrocarbon and type of transfer. Because the off-gas is an air–hydrocarbon mixture, the potential for creating an explosive composition has to be considered in the design of the membrane vapor recovery system. Hydrocarbon vapor–air mixtures containing from 3 to 15% hydrocarbon are in the flammable range. Below 3% hydrocarbon vapor, the mixture is too hydrocarbon-lean to burn. Above 15% hydrocarbon vapor, the mixture does not contain enough oxygen to burn. Problems occur in the intermediate range, where a chance spark can cause an explosion. The usual solution to this problem is to saturate the incoming feed mixture with additional hydrocarbon vapor in a small contactor tower. This ensures that the feed to the compressor needed to operate the membrane unit is always comfortably above the upper explosion limit, regardless of the composition of the feed gas. As an additional safeguard, liquid-ring compressors are usually chosen. In a liquid-ring compressor, the seal between the rotating vane of the compressor and the compressor chamber is formed by a film of liquid—in this case, liquid gasoline. The liquid seal minimizes metal-to-metal contact and the possibility of sparks. As the gas is compressed, some hydrocarbon

vapor is absorbed by the gasoline sealing fluid of the compressor. The fluid leaving the compressor is then a two-phase mixture of gasoline containing dissolved vapors and hydrocarbon-saturated air. A phase separator, after the compressor, separates the hydrocarbon liquid and gas phases. The vapor-saturated gasoline is removed; the saturated vapor then passes to the membrane unit. As with the condensation–membrane separation unit. Hydrocarbon vapors are removed by using a hydrocarbon- selective membrane. The hydrocarbon-enriched permeate is recycled to the front of the feed gas compressor; the hydrocarbon-stripped residue contains 0.5–2% hydrocarbon, mainly the light gases methane, ethane, and propane. To meet air discharge regulations, this gas is usually sent to a final polishing step, most commonly a small, molecular sieve, pressure swing absorption (PSA) unit, which reduces the hydrocarbon level to 0.2– 0.5 vol%. The gas under treatment passes through the flammable range from the hydrocarbon-saturated feed (5–10% hydrocarbon) to the hydrocarbon stripped residue (0.5–2% hydrocarbon) within the membrane module. Since there are no moving parts within the module, the chance of a spark causing an explosion is minimal. GKSS’s licensees have installed about 30 gasoline vapor recovery systems at fuel transfer terminals, mostly in Europe. The alternative technology is to use some sort of thermal oxidizer, and this approach seems to be the most widely used technology, especially in the United States. A related gasoline vapor recovery application in which membranes are finding it easier to compete is at retail gasoline stations. Many new gasoline stations are using vacuum-assisted dispensing systems to control the release of hydrocarbon vapors to the atmosphere. These systems use a small pump to draw air and vapors from the gasoline dispensing nozzle. For every liter of gasoline dispensed, as much as 2 L of air and gasoline vapor are returned to the storage tank. The air that builds up in the tank must be vented to the atmosphere. Membrane systems are used to control the vapor emissions. In the last few years, several hundred retail gasoline stations have installed small membrane systems to treat their tank vents (see figure 2.2). Air from the gas station dispenser is collected and sent to the gasoline storage tank. When the pressure in the tank reaches a preset value, a pressure switch activates a small compressor that draws off excess vapor-laden air. A portion of the hydrocarbon vapors condense and is returned to the tank as a liquid. The remaining hydrocarbons permeate the membrane and are returned to the

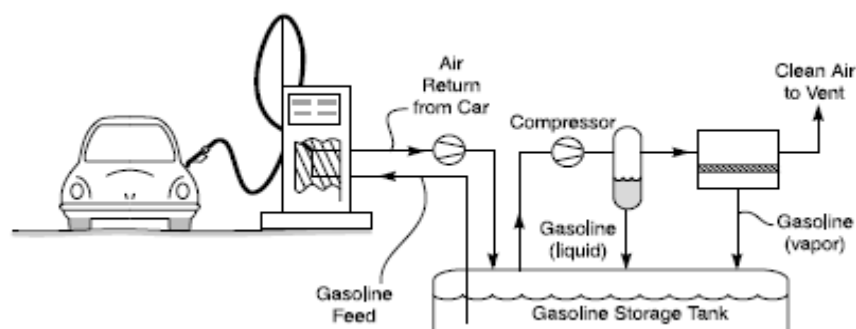


**Figure 2.2:** Flow diagram of a membrane gasoline-vapor recovery unit suited to a retail gasoline station tank vent.

tank as concentrated vapor. Air, stripped of 95–99% of the hydrocarbons, is vented. In addition to eliminating hydrocarbon emissions, the unit essentially pays for itself with the value of the recovered gasoline. Typical systems are small, containing a single 1- to 2-m<sup>2</sup> membrane module and costing from \$5000 to 15,000. Several hundred, perhaps as many as 1000, of these systems have been installed around the world [53].

Another key important area of gas separation in which membranes are involved is the refining of natural gas. Raw natural gas is often saturated with propane, butane, higher hydrocarbons, and water. Separation of these components is necessary to prevent formation of hydrocarbon liquids and hydrates in the pipeline, as well as to control Btu (British thermal unit) content. In addition, their removal is desirable on economic grounds; the hydrocarbons have more value as recovered natural gas liquids (NGLs). Membranes can be used to bring raw natural gas to pipeline quality by removing water and higher hydrocarbons. A simple, economical membrane system can lower the dew point of the gas by 80–120 EF (30–508C). The current alternative technology cools the gas using a refrigeration unit and separates the heavy hydrocarbons by condensation. Thus far, membrane systems have had difficulty replacing refrigeration for removing heavy hydrocarbons from large-volume gas streams, but a number of membrane units have been installed to treat gas used as on-site fuel for remote gas compressor engines [54].

Raw unprocessed natural gas is widely used to power field compressor engines and generator sets. Oftentimes this gas has a low octane rating because of the presence of propane and C4þ hydrocarbons in the gas. These components lead to predetonation and coking problems, requiring derating of the engines so that they can run smoothly. Engine and turbine manufacturers characterize the quality of natural gas in a number of

ways, most commonly by calculating the methane number, or Wobbe number, of the gas. These numbers are equivalent to the octane rating used to characterize gasoline. Good gas has a methane number of greater than 65; a methane number of 40 or below can be used as engine fuel but will usually require derating of the engine. Another measure of gas quality is its Btu value. Below 600–700 Btu/scf, gas is considered very lean; above 1200 Btu/scf, gas is normally too rich to be used in standard gas-powered equipment. Finally, most engine manufacturers will have a limit on the hydrogen sulfide content of the gas. The amount of gas used by field engines is usually in the 0.5–2.0-MMscfd (million standard cubic feet per day) range—too small to make treatment of the gas by refrigeration economical. As a consequence, many engine users are forced to live with the problem gas and the resulting low reliability and high maintenance costs.

Currently, the total membrane vapor separation equipment market is at least \$20–30 million/year and growing and diversifying. Although these statistics are unlikely to excite most venture capitalists, the creation of a new market segment in the conservative world of chemical engineering is an unusual achievement. The modest but solid growth of market share for membranes over the last 15 years and the opportunities for development of new product lines are optimistic indicators for a bright future.

#### **2.2.2.4 Membranes for environmental applications**

Separations using synthetic membranes have been widely adopted for environmental applications. In this area the key claim is the recovery of metals from aqueous solutions. Heavy metals are a kind of contaminant that must be taken into account. They are very toxic for both humans and aquatic fauna and flora. This is the reason why it is very important their removal. There are severe rules about their elimination from wastewaters before discharge into the environment and also from drinking water. The membranes usually utilized for the removal of metals are the so-known as supported liquid membranes (SLMs). In SLMs, the liquid membrane phase is the organic liquid imbedded in pores of a microporous support. When the organic liquid contacts the microporous support, it readily wets the pores of the support, and the SLM is formed. For the extraction of a target species from an aqueous feed solution, the organic-based SLM is placed between two aqueous solutions, the feed solution and the strip solution, where the SLM acts as a semipermeable membrane for the transport of the target species from the feed solution to the strip solution. The organic in the SLM is immiscible in the aqueous feed and strip streams and contains an extractant, a diluent



that is generally an inert organic solvent, and sometimes a modifier. In both types of liquid membranes, facilitated transport is the mass transfer mechanism for the target species to go from the feed solution to the strip solution. The use of SLMs for the removal of metals, including chromium [55,56], copper [57] zinc [56,57] cobalt [56,58,59] and strontium [56,60], from aqueous solutions and wastewaters has long been pursued by the scientific and industrial community. Although an SLM process is very effective for the removal of trace contaminants to very low levels due to its ability to circumvent equilibrium limitation, its use has been hampered by its stability. The traditional SLM suffers from a gradual loss of the organic membrane phase to the aqueous feed and strip solutions, due to emulsification (e.g., resulting from lateral shear forces) at the membrane–aqueous interfaces and to the osmotic pressure difference across the membrane. The osmotic pressure difference displaces the organic membrane phase from the micropores of the support. Displacement of the organic membrane phase from the pores can ultimately allow mixing of the feed and strip solutions, leading to complete failure of the separation unit.

## **2.3 Molecularly imprinted membranes (MIMs): An overview**

A MIM is a membrane either composed of a MIP (Molecularly Imprinted Polymer) or containing a MIP. Utilisation of MIPs in MIMs separation was firstly proposed by Piletsky at the beginning of the 90s. Since that MIMs technology has been extensively developed and applied in numerous areas.

### **2.3.1 MIM preparations strategies**

Nowadays the main strategies stabilised for the preparation of MIMs can be divided as follows:

- \*Sequential approach- Preparation of membranes from previous presynthesized MIPs .
- \*Simultaneous formation of MIP structure and membrane morphology. Once established the MIP synthesis protocols the synchronisation of imprinting and films solidification are of central importance for MIP shape morphology structure and function. Two main routes towards MIM are used : “Traditional” in situ cross linking polymerisation and “alternative” polymer solution phase inversion

\*Sequential approach- preparation of MIPs on or in support membranes with suited morphology.

#### **2.3.1.1 From pre-synthesized MIPs to MIMs**

Only a few attempts from presynthesized MIP to separation membranes have been reported. A promising example is the arrangement of MIP nanoparticles as a filter cake between two microfiltration membranes; these flat-sheet filters have been evaluated respect to their flow and binding [61,62]. The actual tendency in the preparation of this kind of MIMs is the dispersion of MIPs into a polymeric stable matrix and subsequent membrane preparation by phase separation. This kind of MIMs are essentially more stable in practically all organic solvents than conventional MIMs and offer better experimental results. Numerous work concerning this “hybrid” MIMs have been proposed [63,64].

#### **2.3.1.2 Simultaneous formation of MIP and membrane structure: Crosslinking polymerisation**

In an early study, the crosslinking copolymerization of a mixture of acrylamide and acrylates including a photo-isomerizable functional acrylate yielded a MIM with a poor mechanical stability due to the swollen structure [65]. To adapt MIP to synthesis of flat-sheet membranes free standing but brittle MIM have been prepared by thermally initiated in situ crosslinking copolymerization of one of the standard monomer mixtures (MAA/EDMA) [66]. A significant improvement have been achieved by using oligourethane-acrylate macromonomer in in situ imprinting polymerization mixtures in order to increase the flexibility and mechanical stability of membranes; self supported MIM with with a thickness between 60 and 120  $\mu\text{m}$  have been prepared [67]. One approach to obtain more permeability was the use of a macromolecular pore former (polyester) along with cross-linking copolymerization of styrene monomers [68].

#### **2.3.1.3 Simultaneous formation of MIP and membrane structure: Polymer solution phase inversion (PI)**

Consist in polymer solution casting films and subsequent precipitation by two ways: Solvent evaporation or immersion of precipitation. Using solvent evaporation, also called “dry PI”, the solvent is evaporated and as a consequence the polymer precipitates. Using immersion of precipitation, also called “wet PI”, the casting solution is immersed

in a coagulation bath. The coagulation bath is composed by “non solvent” in which polymer is not soluble and have affinity by the solvent used in synthesis of polymer. The molecules of solvent are exchanged by molecules of non solvent causing polymer precipitation. Yoshikawa for example used polystyrene resins with peptide recognition groups , in a blend with a matrix polymer, for the MIM formation via “dry PI” by solvent evaporation [69-71]. Remarkably, the permeability was much higher for the MIM as compared with blank membranes.

Alternatively Kobayashi used functional acrylate copolymers for “wet PI” giving asymmetric porous MIM by immersion precipitation [72-74]. The copolymer material and methodology have been adapted by another group[75] .The polymer selection for phase inversion imprinting have been extended to most of the commonly used membrane materials e.g cellulose acetate [76], polyamide [77], polyacrilonitrile [78] and polysuphone [79]. The formation of porous MIM from a compatible blend of a matrix polymer—for adjusting a permanent pore structure—and a functional polymer—for providing binding groups—could provide even more alternatives [80]. Furthermore, polyethyleneglycol as pore former in the polymer blend casting solution had been successfully used to increase the membrane permeability [80] . A “hybrid” approach of in situ polymerization and “wet PI” had been also reported: The polymerization of functional monomers had been performed in the presence of the template, and the resulting solution of *linear* copolymers, either P(AN-co-AA) or P(AN-co-MAA), with the associated template had then been directly used for film casting/immersion precipitation towards porous MIM [81]. However, the membranes have only been characterized in batch sorption experiments. It is remarkable, that most MIM prepared via phase inversion imprinting had at least acceptable binding performance in aqueous media. However, such MIM lost their “template memory” when exposed to a too organic environment where swelling and chain rearrangement seemed to “erase” the imprinted information. However, it should be noted, that even if the PI should be most suited for the preparation of separation membranes, the adaptation of the process to the preparation of MIM is complicated because the conditions required for an optimal formation of MIP sites may not be compatible with the ones for obtaining an optimal pore structure.

Furthermore, the type of pore structure—e.g. symmetric macroporous or microporous versus asymmetric—will have decisive impact onto MIM separation performance. all simultaneous preparations share the same major problem, that MIP sites and membrane

morphology are formed in the same step from the same building blocks, either monomer or polymers. Therefore, the limited accessibility of imprinted sites due to a random distribution inside and on the surface of the bulk polymer phase remains a major unsolved problem. Furthermore, the problem of combining a high yield of MIP sites with a pore structure suited for efficient membrane separation had not yet been solved.

#### **2.3.1.4 Preparation of composite MIMs**

Advanced molecular separations, e.g. via reverse osmosis, nanofiltration, pervaporation or membrane adsorption, are performed using composite membranes, where an optimized porous support membrane is functionalized with a suited thin selective layer. Analogously, the preparation of MIP composite membranes should allow adjust membrane pore structure and MIP recognition sequentially and by two different materials. In the earliest attempts, established MIP synthesis mixtures, e.g. MAA/EDMA, had been polymerized in mm-thick glass filters to fill their pores [82,83]. Later, reaction mixtures had been casted into the pores of a symmetric microfiltration membrane and a cross-linking copolymerization of a functional polyacrylate had been performed [84]. In both cases, thick symmetric MIM had been obtained, with the mainly meso- and microporous MIPs filling all pores of the support material. Thin film MIP composite membranes, with a minimized thickness of the MIP layer acting as selective barrier, should enable a much higher membrane permeability. With that intention, in situ photoinitiated crosslinking copolymerization of a MAA/EDMA mixture had been performed on top of an asymmetric 20 nm pore size alumina membrane [85]. Also, a cellulosic dialysis membrane had been used as matrix for a two-step grafting procedure yielding a MIP by in situ copolymerization in the thin mesoporous barrier layer of the base material [86]. Macroporous composite membranes, evenly functionalized with thin MIP layers, had been developed to achieve high performance MIM adsorbers [87-90]. The structure of the base membrane can be used as a means to adapt both pore size—permeability—as well as internal surface area—binding capacity—to the desired application. Using a coated photoinitiator, a photo-initiated cross-linking graft copolymerization yielded very thin MIP films which were covalently anchored and covered the entire surface of the base membrane [88]. Based on the results of surface and pore analyses, the thickness of MIP layers with the highest

affinity and selectivity was below 10 nm . Moreover, it had been discovered that a previously prepared thin hydrophilic layer on the support membrane can have two functions [89]:

- (i) matrix for the crosslinking polymerization and limiting monomer conversion to “filling” the layer thus forming an interpenetrating polymer network,
- (ii) (ii) minimizing non-specific binding during SPE. A superior MIM performance, especially a high template specificity, could be achieved using this advanced composite structure.

The sequential approach will allow to use the base membrane pore structure (barrier pore size) and layer topology (symmetric versus asymmetric) as well as the location of the MIP—on top of (“asymmetric”) or inside (“symmetric”) the support membrane—to prepare different MIM types, with the MIP either as selective barrier or transport phase or as an affinity adsorber layer.

### **2.3.2 MIMs Separations.**

The template binding to MIP sites in a MIM can be coupled with a selective transport through the MIM thus enabling a membrane separation. The transport pathways in a polymer membrane can be either the free volume between polymer chains, the solvent fraction of a swollen polymer gel or connected pores in a solid polymer. Two major mechanisms for selective transport can be regarded:

- (a) Facilitated permeation driven by preferential sorption of the template due to affinity binding—slower transport of other solutes,
- (b) Retarded permeation due to affinity binding—faster transport of other solutes, until a saturation of MIP sites with template is reached.

In case (a), depending on the membrane structure as well as MIP site concentration and distribution, transport can occur via carrier-mediated (“facilitated”) transport, in real membranes coupled with diffusion [91]. Due to the coupling with non-selective diffusion, separation selectivity can only be achieved for relatively small diameters of trans membrane pores. Note, that most synthetic carrier membranes based on facilitated transport are liquid membranes, i.e. they have a non-porous barrier structure.

In case (b), due to the saturation behaviour, separation efficiency will be mainly determined by MIP binding capacity. Because selectivity is caused by specific adsorption, those MIM can be considered as membrane absorbers [92].

Moreover, the template binding can also change the barrier properties of the MIM, e.g. via an altered membrane swelling. Obviously, the magnitude of such effects will also depend very much on the barrier pore size.

For conventional synthetic membranes functioning according to the solution–diffusion mechanism, such phenomena are well-known: The sorption of the preferred solute in the membrane will lead to a swelling thus also enabling the transport of other less preferred solutes, causing a reduced membrane separation selectivity[93]. With MIM, however, the effect will be specific with respect to the imprinted site receptor function: The resulting response, a changed membrane permeability, can be used for separation but also as a transducer in a sensor system or for controlled release through a membrane. Hence, for tailoring and optimizing MIM function, it is critically important to control the affinity of MIP sites along with their density in the membrane and to create a well-defined membrane pore morphology.

### **2.3.2.1 Mechanisms for transport and selectivity**

A detailed pore morphology analysis have not yet been performed for the MIM with mainly meso- and microporous barrier. The conclusions from permeability and other data for MIM and blank membranes [69,83,85] can be summarized as follows:

- \* no large transmembrane pores exist in MIM and blank membranes (the membranes described by Kimaro et al., [68] where additional pores had been created with help of a pore former, are an exception; however, in these MIM the large pores represented only very low surface and volume porosities),
- \* imprinting creates a specific micropore fraction in MIM which is not present in the blank membranes,
- \* imprinting can contribute to the connectivity of pores.

Microporous MIM's permselectivity is based on preferential and reversible binding and exchange between template and MIP sites in the membrane thus providing pathways for selective trans-membrane transport. However, the different behaviour of membranes from different materials and preparation methods, imprinted for various templates and studied under various conditions, demonstrates the need for further detailed investigations of membrane structure as well as detailed transport characterization of well-defined membranes from controlled preparations, with a particular focus on dynamic effects onto micropore structure.

### **2.3.3 Performance of microporous MIMs**

Microporous MIM performance must be compared with established membranes for molecular separations, mainly for ultrafiltration, dialysis, nanofiltration or reverse osmosis. If the fluxes through MIM could be increased without compromising the selectivity and if this performance could be maintained for a long time under technical conditions, such novel materials could immediately gain practical relevance. Imprinting efficiency, membrane morphology and separation conditions can be further optimized in order to improve the selective flux. It is most promising that significant binding and transport selectivities can also be achieved by imprinting with rather common functional Polymers [76-78,80,81]. In terms of membrane morphology, the potential of thin-layer composite MIM for increasing permeability has already been indicated[85,86]. Imprinting efficiency and membrane morphology can most efficiently be addressed by tailored composite membranes, i.e. using the sequential preparation approach. An example is filling the straight and regular pores of thin track-etched membranes with MIPs [94]. Also, the evidence for a positive impact of a higher driving force onto flux *and* selectivity is most interesting [71]. In conclusion, advanced MIM which enable a continuous and truly molecule-selective separation based on affinity interactions seem to be feasible and could have a very large application potential.

### **2.3.4 Macroporous MIM-MIP as affinity absorber layer**

With macroporous membranes, molecular separations can only be achieved via interactions with the membrane material. Convective flow through the membrane can be used as means to improve separation performance via elimination of diffusion resistances. The advantages of membranes in comparison with other absorbers such as beads are a high selective binding capacity at a high throughput [95]. With MIM, the molecule selectivity could be tailored by the binding affinity of imprinted sites, i.e. the efficiency of molecular imprinting. However for MIM as for any other membrane absorber, pore morphology is of major importance: The micropore fraction will determine the binding capacity, and a connected macropore fraction will be essential for efficient trans membrane transport and elimination of diffusion resistance.

#### **2.3.4.1 MIP particles composite membranes**

MIP particle composite membranes, with a macroporous void fraction and a rather symmetric layer topology, had been studied as absorbers. Especially, the use of monodisperse particles is very promising because a rather even flow distribution could be achieved. However, permeabilities and binding site accessibility were relatively low so that the binding studies had been performed by recirculating the analyte solution through the membrane for many hours in order to achieve the plateau values.

#### **2.3.4.2 Thin layer MIP composite membranes**

Due to the macroporous structure of the support microfiltration membrane, thin-layer MIP composite membranes for herbicides could be characterized at very high flow rates [88-90]: The *dynamic* binding capacities obtained in one fast filtration step (less than 10 min.; i.e. without any recirculation), normalized to the amount of functional polymer, were similar to the *static* binding capacities for the best phase inversion MIM[70]: For example, the thin-layer MIP PVDF composite membranes had a degree of grafting of 340 g/cm<sup>2</sup> [89], so that the observed 13 nmol/cm<sup>2</sup> MIP-specific binding capacity (measured at a terbumeton concentration of only 10 µmol/l) correspond to 38 µmol/g. For the advanced composite MIM a very high selectivity, e.g. a separation factor of 15 for terbumeton versus atrazin, had been achieved [89]. Furthermore, quantitative template recovery by elution from the MIM was possible, and the MIM were reusable in several subsequent bind-wash-elute cycles [88]. Currently, the main objective is further improving the MIM binding capacities [94]. The high MIM permeabilities would enable an efficient isolation or removal of a dilute valuable or toxic compound from a very large volume like in the case of this thesis.

#### **2.3.5 Performance of macroporous MIMs**

Performance of macroporous MIM should be discussed in the context of affinity membrane absorbers which itself directly compete with other affinity materials, either established, e.g. particles, or alternative ones, e.g. monoliths [95]. For the first high-flux composite MIM [88-90], binding selectivities are promising but the capacities must still be improved. When compared with commercial affinity membranes using, e.g., ion-exchange groups, MIM—due to the higher spatial order of functional groups in the imprinted sites on the accessible surface—will per se have somewhat lower capacities. However, when compared with membrane-immobilized proteins [96], receptor site



density may even be higher for MIP layers. In order to achieve the performance goals, further improvements of the (sequential) preparation of composite MIM will be the most effective approach. Hence, tailored materials for MIM-SPE could already be envisioned. Further applications, e.g. in membrane chromatography [95] or in lab-on-a-chip devices, will follow [97].

### **2.3.6 Combinations of novel MIP formats with membrane separations**

Active development is devoted to the synthesis of MIPs as nanoparticles [98-100] or even microgels [101,102]. With small particles of well-defined morphology in a colloidal dispersion, the specific binding capacity of MIPs can be increased significantly. Ultimately, with microgels not only the function of the binding site but also the three-dimensional structure of biomacromolecules can be mimicked, because the MIP microgels have a molecular weight in the same range as that of proteins. However, the handling of such small entities requires mechanisms which are suited for colloids or biomacromolecules. In that context, “conventional” separation membranes become increasingly attractive. In fact, during the first syntheses of MIP nanoparticles or microgels and during the evaluation of their binding properties, ultrafiltration has already been used as an alternative to (ultra)centrifugation for particle purification and separation. Consequently, similar to the rapid development of affinity membrane processes for separation and reaction engineering [103,104], the integration of MIP particle and membrane technologies will be extended towards batch, semi-batch and continuous separator and reactor systems. Those Systems will be either based on a rather simple combination of MIPs and membranes, for retaining nano-MIPs in the system by a membrane, or on the immobilization of nano-MIPs in membranes with suited transport properties. The latter composite membranes could be developed towards tailored separation membranes, e.g. using MIP microgels as fixed or even mobile carriers, or towards catalytically active membranes based on the immobilization of enzyme-mimicking MIPs.

### **2.3.7 Final Remarks**

The unique feature of MIM is the interplay of selective binding and transmembrane transport of molecules, making them potentially superior to state-of-the-art synthetic separation membranes already applied in various industries. Receptor and transport

properties of microporous MIM can be based on template-specific binding sites in trans-membrane pores, which serve as fixed carriers for “facilitated” transport. Furthermore, template binding in microporous MIM can lead to a “gate effect” which either increases or decreases membrane permeability. Alternatively, MIM can also function as adsorbers, leading to a retardation of template transport followed by breakthrough once the binding capacity has been saturated. Finally, the development of nano-MIPs will facilitate other synergistic combinations with separation membranes for effective separations based on MIPs. The existing data in the literature can be considered as the “proof-of-feasibility” for separations with MIM, but much further work will be necessary to really explore their potential. A better integration of the fundamental knowledge about membrane materials and technology from the last decades will provide guide-lines for the development of improved MIM with tailored and stable selectivities for diverse separations. These properties must be combined with a high membrane permeability. Therefore, significantly advanced preparation methods and a much more detailed structure characterization will be necessary in order to be able to rationally design permselective MIM. The main problem in MIM preparation is to optimize MIP recognition and membrane transport properties at the same time. The most promising routes are innovative strategies based on novel materials, e.g. polymer blends, block copolymers or inorganic/organic composites, and the preparation of composite membranes. Towards improved composite membranes, surface functionalization—by self-assembly or controlled grafting—can be used for either coating the pore surface or a controlled filling of pores. Pore-filling applied to asymmetric ultrafiltration membranes, could ultimately enable the application of the MIP “gate effect” for efficient separations via “smart” membranes. Also, the use of presynthesized MIPs for composite membranes, either via creating filter beds from nanoparticles or via entrapment or other immobilization of nano-particles or micro-gels in filter structures, should be explored in more detail.

Once MIM materials with attractive intrinsic properties will have been obtained, module and process design will be the next critical issues. In particular for separations by microporous MIM with low permeability, the preparation of hollow-fibre membranes could serve as a means to increase the membrane area per volume of a separation unit. For higher driving forces and long term operations, problems with concentration polarization and membrane fouling must be solved. All these challenges can be met by adapting the knowledge in “conventional” membrane technology

[105,106]. Moreover, the integration of membranes, as separation media or for process intensification, in lab-on-a-chip systems is already underway [97].

Among first examples for real applications will be MIM absorbers for the specific sample enrichment from large volumes by membrane SPE, and for the specific decontamination of large process streams. However, the already demonstrated ease of integrating separation membranes into high-throughput technologies, will at the same time facilitate the use of substance-specific MIM or MIM libraries in screening applications. Other promising continuous separations are the resolution of enantiomers or the (by) product removal from bioreactors, both feasible either by electrodialysis or by dialysis. Controlled release or delivery from or through MIM, including fibres or capsules, will be another field of attractive potential applications. Targets could be drugs but also technically or environmentally interesting substances. Release from MIP-based depots could occur passively, with the MIM as barrier dictating the transport kinetics, but also triggered by a stimulus from the environment, e.g. via recognition of a specific signal molecule at an imprinted site.

In a more general context, MIM can serve as model systems for cellular transmembrane transport and natural receptors. Applications in sensors can be immediately derived from those models. MIP films have already been adapted to various sensor and assay formats [107], fulfilling the minimum requirement—immobilization of the receptor—but also

fitting to the need of various detection formats. For the integration of transducer functions into MIP films, the use of membrane transport effects.

may be especially beneficial for implementing improved detection specificity and signal amplification. Biocompatibility of materials in contact with cells or tissue, relies on specific molecular recognition processes, especially at the interfaces, and imprinted surfaces are expected to play a key role in this field in the future [108]. Thin-layer MIP composite membranes for the recognition of proteins, but also for cell-specific recognition based on surface-marker structures or cell shape could also be envisioned. Ultimately, catalytic MIM, integrating and organizing separation and reaction in space and time, have a great perspective as key elements for advanced “bio-mimetic” processes in chemical and biochemical reaction engineering [109].

## References

- [1] Wulff, G., Sarhan, A., *Angew. Chem. Int. Ed. Engl.* (1972) 11, 341.
- [2] Mosbach, K., *Trends Biochem.* (1994) 19, 9.
- [3] Caro, E., Masque, N., Marce, R.M., Borrull, F., Cormack, P., Sherrington, D.C., *J. Chrom. A.* (2002) 963,169.
- [4] Ye, L., Mosbach, K., *J. Incl. Phenom. Macrocyclic. Chem.* (2001) 41, 107.
- [5] Lieberzeit, P.A., Dickert, F.L., *Anal. Bioanal. Chem.* (2008) 391, 1629.
- [6] Rachkov, A., McNiven, S., El'skaya, A., Yano, K., Karube, I., *Anal. Chim. Acta.* (2000) 405, 23.
- [7] Alizadeh, T., *Anal. Chim. Acta.* (2008) 623, 101.
- [8] Lin, Y., Tang, S.Q., Mao, X., Bao, L., *J. Biomed. Mater. Res. A* (2008) 85, 573.
- [9] Khan, H., Khan, T., Park, J.K., *Sep. Purif. Tech.* (2008) 62, 363.
- [10] Maier, N.M., Lindner, W., *Anal. Bioanal. Chem.* (2007) 389, 377.
- [11] Ye, L., Haupt, K., *Anal. Bioanal. Chem.* (2004) 378, 1887.
- [12] Volkmann, A., Bruggemann, O., *React. Funct. Polym.* (2006) 66, 1725.
- [13] Mulder, M., *Basic Principles of Membrane Technology*, second ed., Kluwer Academic Publishers, (1996).
- [14] Ho, W., Sirkar, K.K., *Membrane Handbook*, Kluwer Academic Publishers, Dordrecht, (1992).
- [15] Bechhold, H., *Z. Phys. Chem.* (1907) 60, 257.
- [16] Elford, W.J., *Trans. Faraday Soc.* (1937) 33, 1094.
- [17] Zsigmondy, R., Bachmann, W., Über Neue Filter, *Z. Anorg. Chem.* (1918) 103, 119.
- [18] Ferry, J.D., *Chem. Rev.* 18, 373 (1936).
- [19] Loeb, S., Sourirajan, S., *Advances in Chemistry.* (1963) 28, 117.
- [20] Kurihara, M., Uemura, T., Himeshima, Y., Ueno, K., Bairinji, Y., *Nippon Kagaku Kaishi* (1994) 2, 97.
- [21] Yamamura, H., Kurihara, M., Maeda, K., (1994). *Japanese Patent Applications* H06-245184 and H08-108048.
- [22] Ohya, H., Suzuki, T., and Nakao, S., *Bull. Soc. Sea Water Sci. Japn.* (1996) 50, 389.
- [23] Fukunaga, K., Matsukata, M., Ueyama, K., and Kimura, S., *Membrane*, (1997) 22, 211.

- [24] World Health Organization (WHO) (2004). *Guidelines for Drinking Water Quality*, 3rd ed. WHO, Geneva.
- [25] Rodriguez, M., Ruiz, A. F., Chilon, M. F., Rico, D. P. (2001) *Desal.* 140, 145.
- [26] Toray. Brochure of TM800, (2004) Tokyo, Japan.
- [27] Redondo, J., Busch, M., and Witte, J. D., *Desal.* (2003) 156, 229.
- [28] Hiro, A., and Hirose, M., *Nitto Giho* (2000) 40, 36.
- [29] Taniguchi, M., Fusaoka, Y., Nishikawa, T., and Kurihara, M., *Desal.* (2004) 167, 419.
- [30] Bassett, P., *Tissue Engineering: Technologies, Markets and Opportunities*, (2001) 3rd ed. D&MD Report.
- [31] Dai, N.T., Williamson, M. R., Adams, E. F., Coombes, A. G. A., and Khammo, N., *Biomat.* (2004) 25, 4263.
- [32] Danielsson, C., Ruault, S., Basset-Dardare, A., Frey, P., (2006). *Biomat.* 27, 1054.
- [33] Choo, A., Padmanabhan, J., Chin, A., Fong, W. J., Oh, S. K. W.. *J. Biotech.* (2006) 122, 130.
- [34] Nagase, K., Kohori, F., and Sakai, K.. *Biochem. Eng. J.* (2005) 24, 105.
- [35] Wickramasinghe, S. R., Garcia, J. D., Han, B.. *J. Membr. Sci.* (2002) 208, 247.
- [36] Strathmann, H., *Am. Inst. Chem. Eng. J.* (2001) 47, 1077.
- [37] Saito, A., Suzuki, H., Bomszyk, K., Ahmad, S., *Mater. Sci. Eng. C* (1998) 6, 221.
- [38] Krasteva, N., Harms, U., Albrecht, W., Seifert, B., Hopp, M., Altankov, G., Groth, T., *Biomat.* (2002) 23, 2467.
- [39] Flendrig, L.M., Soe, J. W., Jorning, G. G. A., Steenbeek, A., Karlsen, O. T., Bovee, W. M. M. J., Ladiges, N. C. J. J., te Velde, A. A., and Chamuleau, R. A. F. M.. *J. Hepatol.* (1997) 26, 1379.
- [40] Ye, H., Xia, Z., Ferguson, D. J. P., Triffitt, J. T., Cui, Z., *Cytotherapy* (2004) 6, 276.
- [41] Ellis, M. J., and Chaudhuri, J. B., *Biotechnol. Bioeng.* (2007) 96, 177.
- [42] Przybycien, T. M., Pujar, N. S., and Steel, L. M., *Curr. Opin. Biotechnol.* (2004) 15, 469.
- [43] van Reis, R., and Zydney, A.. *Curr. Opin. Biotechnol.* (2001) 12, 208.
- [44] Ghosh, R., *Protein J. Chromatogr. A.* (2002) 952, 13.
- [45] Saksena, S., Zydney, A. L., *Biotechnol. Bioeng.* (1994) 43, 960.
- [46] van Eijndhoven, R. H. C. M., Saksena, S., Zydney, A. L., *Biotechnol. Bioeng.* (1995) 48, 406.

- [47] van Reis, R., Gadam, S., Frautschy, L. N., Orlando, S., Goodrich, E. M., Saksena, S., Kuriyel, R., Simpson, C. M., Pearl, S., Zydney, A. L., *Biotechnol. Bioeng.* (1997) 56, 71.
- [48] Ghosh, R., Wan, Y., Cui, Z. F., and Hale, G., *Biotechnol. Bioeng.* (2003) 81, 673.
- [49] DiLeo, A. J., Allegrezza, Jr., A. E., Builder, S. E., *Biotechnol.* (1992) 10, 61.
- [50] van Holten, R. W., Autenrieth, S., Boose, J. A., Hsieh, W.T., Dolan, S., *Transfusion* (2002) 42, 999.
- [51] Ohlrogge, K., Rockmiller, J. B., Wind, J., Behling, R. D., *Sep. Sci. Technol.* (1993) 28, 227.
- [52] Ohlrogge, K., Stürken, K., *Membrane Technology.* (2001) Wiley, Chichester, Part II p. 71.
- [53] Ohlrogge, K., Wind, J., (2000) *U.S. Patent* 6,059,856.
- [54] Fenstermaker, R. W., (1983). *Engine U.S. Patent* 4,370,150.
- [55] Yang, X. J., Fane, A. G., MacNaughton, S., *Water Sci. Technol.* (2001) 43, 341.
- [56] Ho, W. S. W.,. *Advanced Membrane Technology*, (2003) New York Academy of Sciences, New York, p. 97.
- [57] Gherrou, A., Kerdjoudj, H., Molinari, R., Drioli, E., *Sep. Sci. Technol.* (2002) 28, 235.
- [58] Gega, J., Walkowiak, W., Gajda, B., *Sep. Purif. Technol.* (2001) 22, 551.
- [59] Alguacil, F. J., *Hydrometallurgy.*(2002) 65, 9.
- [60] Mackova, J., Mikulaj, V., *J. Radioanal. Nucl. Chem.* (1996) 208, 111.
- [61] Lehmann, M., Brunner, H., Tovar, G., *Desalination* (2002) 149, 315.
- [62] Lehmann, M., Brunner, H., Tovar, G., *Chem. Ing. Techn.* (2003) 75, 149.
- [63] Kobayashi, T., Ku, C., Faiza, M., Son, L., *J. Sep. Sci.* (2009) 32, 3327.
- [64] Takeda, K., Kobayashi, T., *J. Memb. Sci.* (2006) 275, 61.
- [65] Marx-Tibbon, S., Willner, I., *J. Chem. Soc., Chem. Commun.* (1994) 46, 1261.
- [66] Mathew-Krotz, J., Shea, K.J., *J. Am. Chem. Soc.* (1996) 118, 8154.
- [67] Sergeeva, T.A., Piletsky, S.A., Brovko, A., Slinchenko, L.A., Sergeeva, L.M., Panasyuk, T.L., Elskaya, A.V., *Analyst* (1999) 124, 331.
- [68] Kimaro A., Kelly, L.A., Murray, G.M., *Chem. Commun.* (2001) 1282.
- [69] Yoshikawa, M., Izumi, J., Kitao, T., Koya, S., Sakamoto, S., *J. Membr. Sci.* (1995) 108, 171.
- [70] Yoshikawa, M., Izumi, J., Kitao, T., Sakamoto, S., *Macromolecules* (1996) 29, 8197.

- [71] Yoshikawa, M., Izumi, J., Kitao, T., *React. Funct. Polym.* (1999) 42,93.
- [72] Kobayashi, T., Wang, H.Y., Fujii, N., *Chem. Lett.* (1995) 56, 927.
- [73] Wang, H.Y., Kobayashi, T., Fuji, N., *Langmuir* (1996) 12, 4850.
- [74] Wang, H.Y., Kobayashi, T., Fukaya, T., Fuji, N., *Langmuir* (1997) 13, 5396.
- [75] Trotta, F., Drioli, E., Baggiani, C., Lacopo, D., *J. Membr. Sci.* (2002) 201,77.
- [76] Yoshikawa, M., Ooi, T., Izumi, J., *J. Appl. Polym. Sci.* (1999) 72,493.
- [77] Reddy, P.S., Kobayashi, T., Abe, M., Fujii, N., *Eur. Polym. J.* (2002) 38, 521.
- [78] Reddy, P.S., Kobayashi, T., Fujii, N., *Eur. Polym. J.* (2002) 38, 779.
- [79] Yoshikawa, M., Izumi, J., Ooi, T., Kitao, T., Guiver, M.D., Robertson, G.P., *Polym. Bull.* (1998) 40, 517.
- [80] Ramamoorthy, M., Ulbricht, M., *J. Membr. Sci.* (2003) 217, 207.
- [81] Kobayashi, T., Fukaya, T., Abe, M., Fuji, N., *Langmuir* (2002) 18, 2866.
- [82] Piletsky, S.A., Dubey, I.Y., Fedoryak, D.M., Kukhar, V.P., *Biopolim. Kletka* (1990) 6, 55.
- [83] Piletsky, S.A., Panasyuk, T.L., Piletskaya, E.V., Elskaya A.V., Levi, R., Karube, I., Wulff, G., *Macromolecules* (1998) 31, 2137.
- [84] Dzgoev, A., Haupt, K., *Chirality* (1999) 11, 465.
- [85] Hong, J.M., Anderson, P.E., Qian, J., Martin, C.R., *Chem. Mater.* (1998) 10, 1029.
- [86] Hattori, K., Yoshimi, Y., Sakai, K., *J. Chem. Eng. Jpn.* (2001) 34, 1466.
- [87] Wang, H.Y., Kobayashi, T., Fuji, N., *J. Chem. Technol. Biotechnol.* (1997) 70, 355.
- [88] Piletsky, S.A., Matuschewski, H., Schedler, U., Wilpert, A., Piletskaya, E.V., Thiele, T.A., Ulbricht, M., *Macromolecules* (2000) 33, 3092.
- [89] Sergeyeve, T.A., Matuschewski, H., Piletsky, S.A., Bendig, J., Schedler, U., Ulbricht, M., *J. Chromatogr. A* (2001) 907, 89.
- [90] Kochkodan, V., Weigel, W., Ulbricht, M., *Analyst* (2001) 126, 803.
- [91] Noble, R.D., *J. Membr. Sci.* (1992) 75, 121.
- [92] Roper, D.K., Lightfoot, E.N., *J. Chromatogr. A* (1995) 702, 3.
- [93] Wijmans, J.G., Baker, R.W., *J. Membr. Sci.* (1995) 107, 1.
- [94] Ulbricht, M., Belter, M., Langenhagen, U., Schneider, F., Weigel, W., *Desalination* (2002) 149, 293.
- [95] Svec, F., Frechet, J.M.J., *Science* (1996) 273, 205.
- [96] Borchering, H., Hicke, H.G., Jorcke, D., Ulbricht, M., *Ann. N.Y. Acad. Sci.* (2003) 984, 470.

- [97] Wang, P.C., DeVoe, D.L., Lee, C.S., *Electrophoresis* (2001) 22, 3857.
- [98] Ye, L., Mosbach, K., *Macromolecules* (2000) 33, 8239.
- [99] Vaihinger, D., Landfester, K., Kräuter, I., Brunner, H., Tovar, G.E.M., *Macromol. Chem. Phys.* (2002) 203, 1965.
- [100] Biffis, A., Graham, N.B., Siedlaczek, G., Stalberg, S., Wulff, G. *Macromol. Chem. Phys.* (2001) 202, 163.
- [101] Zimmerman, S.C., Wendland, M.S., Rakow, N.A., Zharov, I., Suslick, K.S., *Nature* (2002) 418, 399.
- [102] Markowitz, M.A., Kust, P.R., Deng, G., Schoen, P.E., Dordick, J.S., Clark, D.S., Gaber, B.P., *Langmuir* (2001) 16, 1759.
- [103] Gupta, M.N., Roy, I., in: M.N. Gupta (Ed.), *Methods for Affinity-Based Separations of Enzymes and Proteins*, Birkhäuser Verlag, (2002) p. 1.
- [104] Sanchez Marcano, J.G., Tsotsis T.T., *Catalytic Membrane Reactors and Membrane Reactors*, Wiley-VCH, Verlag, Weinheim, (2002).
- [105] Mulder, M., *Basic Principles of Membrane Technology*, second ed., Kluwer Academic Publishers, Dordrecht, (1996).
- [106] Ho W., Sirkar, K.K., *Membrane Handbook*, Kluwer Academic Publishers, Dordrecht, (1992).
- [107] Haupt, K., Mosbach, K., *Chem. Rev.* (2000) 100, 2495.
- [108] Shi, H., Ratner, B.D., *J. Biomed. Mater. Res.* (2000) 49, 1.
- [109] Brüggemann, O., *Biomol. Eng.* (2001) 18, 1.



# **CHAPTER 3**

## **Materials and methods**

### 3.1 Membrane forming polymers

Polyacrylonitrile (PAN) was chosen as base polymer to prepare flat-sheet MIMs with specific molecular recognition properties for the template in organic media. The polymer is made of a stable -C-C-C- chain with laterally -CN- groups having strong dipole moments. Several neighbouring dipoles of the same and or different chains interact by coupling (electrostatic attraction). It is evident that steric hindrance of bulky co-monomers (of an acrylic copolymer) severely interrupt these dipole pairings. PAN differs in many respects from common commercial polymers. Typical properties of PAN are its hardness, stiffness, resistance to most solvents and chemicals, resistance to sunlight, heat, microorganisms, slowness to burn and char, compatibility with polar substances, orientation ability and low permeability to gases [1].

These unique properties are caused by the presence of nitrile groups in the polymer molecules and the resulting highly polar character of acrylonitrile polymer (see figure 3.1).

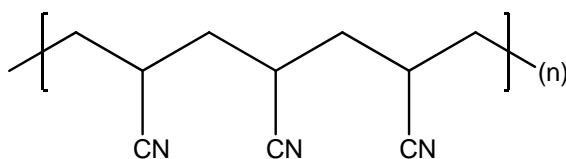


**Figure 3.1:** Chemical structure of PAN

PAN forms hydrogen bonds, transition metal ion complexes, donor-acceptor complexes, and undergoes a number of chemical transformations as well. Even the physical properties of PAN, such as its structure and morphology, are predominantly determined by the interactions of nitrile groups.

It is important also to emphasize that PAN only dissolves in aprotic polar organic solvents such dimethylformamide, dimethylacetamide, dimethyl sulfoxide, sulfolane, ethylene carbonate, and N-methylpyrrolidone. It is also soluble in concentrated sulphuric and nitric acids and concentrated aqueous solutions of some inorganic salts such as lithium bromide, sodium thiocyanate and zinc chloride. During the development of this thesis, it was thought to take profit of PAN properties using this polymer as possible membrane material. In addition some acidic functional groups were also selected to be

introduced into the PAN chains leading different acrylic co-polymers. These co-polymers were effectively used later as the final membrane forming materials. In particular, acrylic acid (AA), methacrylic acid (MAA) and itaconic acid (IA) were the chosen co-monomers. In figure 3.2 are shown the chemical structures of the different synthesised copolymers.

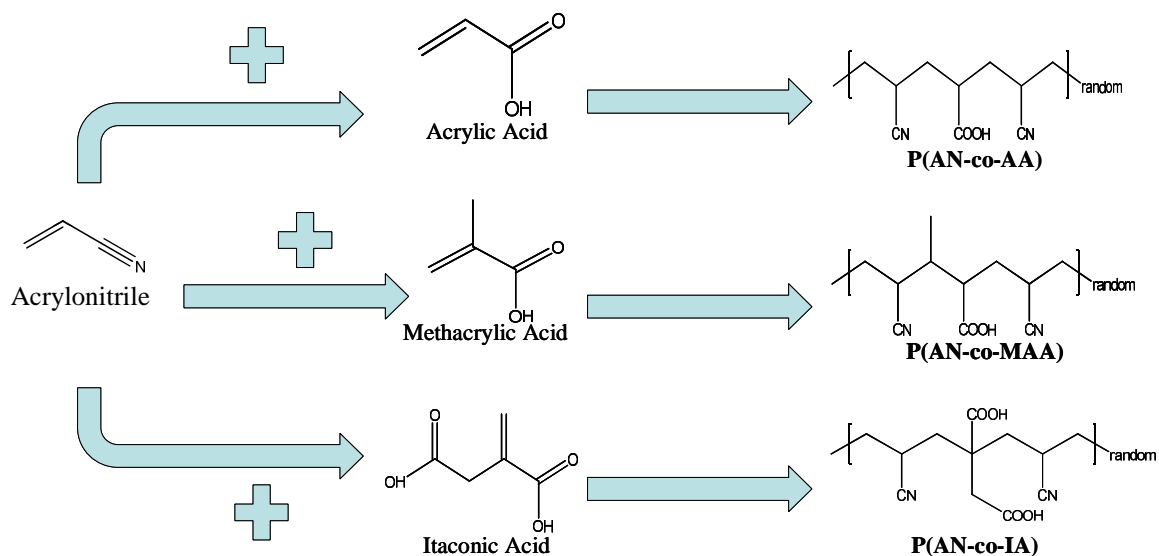


**Figure 3.2:** Chemical structure of co-monomers used and final synthesised copolymers.

### 3.2 Primary amines

Primary amines are chemical compounds used in a considerable number of industries. They are used specially in the manufacture of dyes and pigments. These compounds are also used as intermediates in the preparation of glues, coatings, active pharmaceutical ingredients, polyurethanes and isothiocyanates[2]. Most of them are considered as potentially carcinogens. Since they are used as intermediates reagents in the different steps of synthesis, in many cases they can be found at low concentrations due to a possible un-complete reaction. There is a strict normative and very severe laws in all the industrialised countries concerning the maximum permitted levels of these substances. The target molecule investigated in this work was 4,4'-methylendianiline (MDA). Due to the presence of two aminic groups the possibility to interact via hydrogen bond with acidic functional groups of membranes polymers is still more elevated. Other primary

amines were investigated as structural analogues of MDA and used in selectivity studies. In particular, these molecules were 4,4'-ethylenedianiline (EDA) and single aniline. Figure 3.4 shows chemical structure the different anilines investigated in this work.

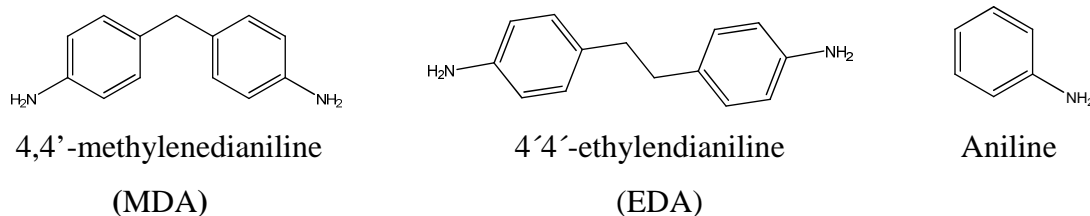


**Figure 3.3:** Chemical structure of the different anilines studied in this work.

The concentration of the different anilines was estimated using a Merk – Hitach D-7000 HPLC device connected to an UV-Vis detector. Previous calibration curves with some standards were also done. Mobil phase used was a mix of acetonitrile-water (55:45). Flow was 1,2 ml/min and absorbance measurements were done at 280 nm. The chromatographic column utilized was the Prevail C-18,5  $\mu\text{m}$  250 x 4,6 mm (Grace). Retention times were 8, 13 and 5 minutes for MDA, EDA and aniline respectively.

### 3.3 Preparation and characterization of polymers

The water-phase precipitation polymerization method was used to carry out the random co-polymerization of AN as main monomer with the previously reported acidic co-monomers. A mixture containing acrylonitrile (AN) and the corresponding acidic co-monomer at wt % ratio of 90/10 was co-polymerized in water at 50 °C during 90 minutes under  $\text{N}_2$  atmosphere and mechanical stirring. The couple  $\text{K}_2\text{S}_2\text{O}_8 - \text{Na}_2\text{S}_2\text{O}_5$  was used as the initiator system in presence of  $\text{Fe}^{+2}$ . The obtained polymers were insoluble in water and precipitated. Then they were filtered and washed many times with fresh water to eliminate possible un-reacted monomers and initiators. With this step the complete purification of the synthesized polymers was achieved. After that, polymers were dried in an oven at 60 °C under vacuum around 24 hour, crushed and ground up into a fine powder. Acidic monomers were introduced into acrylonitrile chains because target molecules under study in this work were aniline having  $\text{NH}_2$  groups. Protons belonging to the acid groups can easily bond by non-covalent

interactions with anilines due to its presence in the solution of imprinted membrane forming polymers. Later, these interactions are supposed to be the key factor in the molecular recognition of target molecule. .

The average molecular weight of the different polymers was determined by intrinsic viscosity measurements of various polymer solutions in dimethylformamide (DMA) using an Ubelode Viscosimeter kept in a bath at 35°C. The average molecular weight of polymers was obtained from the relationship for PAN in (DMA) at 35 °C using the following equation 1:

$$[\eta] = 2.75 \times 10^{-2} M_v^{0.767} \quad (3.1)$$

Where  $\eta$  is the intrinsic viscosity and  $M_v$  is the average molecular weight.

In the other hand FT-IR spectra of synthesised polymers were also done using a Perking Elmer Spectrum One FT-IR spectrometer. The goal was to confirm the introduction of the acidic functional monomers in the acrylonitrile chains.

### **3.4 Preparation and characterization of membranes**

All membranes were prepared from polymer dope solutions in dimethylformamide (DMF). The phase inversion technique was used as membrane preparation method. In particular membranes were prepared by the dry wet process. During the preparation of blank dope solutions only 10% *wt* of each co-polymer was dissolved in DMF. In the other hand, beside 10% *wt* of each co-polymer, 2% *wt* of MDA was added in the case of the preparation of imprinted dope solutions. Polymer solutions were stirred at 50 °C overnight until their complete homogenization and then spread onto a glass support using an casting machine from Elcometer set up with a initial gap of 400  $\mu\text{m}$ . After the glass supports were introduced into an oven at 50 °C causing the partial evaporation of the DMF by approximately 30 mins. Following immersion of glass supports in distilled water caused the formation of membranes. After 30 minutes membranes were transferred in fresh water. Water was changed many times during the following hours to remove eventual DMF remaining traces.

The membrane morphology was investigated by scanning electron microscopy (SEM) images using a Cambridge Stereoscan 360 device, at 20 kV. Membranes permeability in

water and IPA was determined by trans-membrane flux measurements at different pressures in a dead-end filtration cell. The effective working diameter of the membrane was 6.9 cm.

The estimation of the molecular weight cut-off of the prepared membranes was also performed. In this perspective, different rejection tests with some dyes solutions were performed in a dead-end filtration cell already used for the permeability measurements. Initial volume of each solution was 100 mL and the concentration of dye was 10 mg/L. The solution was filtered under stirring through the membrane by the application of pressure of 10 bar. The dye concentration of feed and permeate was determined by spectrophotometric measurements using a Perking Elmer Lambda EZ 201 UV-Vis spectrophotometer. The dye rejection was determined by the equation 4.1:

$$R(\%) = 1 - \left( \frac{C_p}{C_f} \right) \times 100 \quad (4.1)$$

Where: R(%) is the rejection percentage,  $C_p$  and  $C_f$  are the concentrations of dye in the permeate and feed solution, respectively.

The rejection tests were performed using the following dyes: methyl orange bromothymol blue and rose of Bengal. Rejection measurement is one of the most important tests performed to assess the separation properties of membranes [3]. In addition this test allows making an estimation of the average membrane pore size based on the molecular weight of species that permeate through the membrane.

In order to evaluate binding capacities of membranes towards the template MDA, binding experiments were performed measuring sorption of the different anilines from IPA solutions. These experiments were carried out in a dead-end filtration cell already mentioned. Before to start any binding experiments, the removal of target molecule from imprinted membranes was done. In this context, membrane samples were placed in the filtration cell and washed many times with methanol until no traces of target molecule were found in the collected permeate by means HPLC analysis. Using this procedure the target molecule contained into the imprinted membranes was completely extracted.

Each binding experiment consisted in the filtration of 100 ml of MDA solution in IPA at different initial concentration. In all cases, the total amount of MDA retained by the membranes was calculated according the equation 3.2:

$$R_{MDA} = \frac{(C_0 - C_p)V}{m} \quad (3.2)$$

Where:  $R_{MDA}$  is the amount of MDA retained per gram of membrane,  $C_0$  is the concentration of MDA in the feed solution,  $C_p$  is the final concentration in the collected permeate and  $V$  is the volume. The experimental data was reported as the average of three different experiments. Blank membranes were also exposed to the same procedure in order to compare the sorption of non-imprinted membranes.

Initial concentrations studied were 2.5, 5 and 10 mg/L. The goal was to study how initial concentration affected the capacity of the prepared membranes to retain the target molecule during filtration experiments.

In one second investigation the same procedure was followed but using butanol as solvent and filtering 200 ml of 10 mg/L MDA solutions.

In addition, selective properties of P(AN-co-AA) MDA-imprinted membranes were evaluated performing binding tests with other anilines such as EDA and aniline. Chemical structure of EDA is very similar to the template. On the other hand, aniline belongs to the same family but is smaller than the template and possesses only one aminic group.

The selectivity factor ( $\alpha$ ) was calculated using the equation 3.3:

$$\alpha = \frac{R_{template}}{R_{analogue}} \quad (3.3)$$

Where:  $R_{template}$  is the amount of template retained by the imprinted membrane and  $R_{analogue}$  is the amount of the structural analogue retained by the membrane imprinted with the template.

In order to evaluate the influence of the functional co-monomer on the membrane performance, binding tests were also carried out using membranes prepared with the other synthesised copolymers. Results were compared with those obtained with the

P(AN-co-AA) based membranes. In particular, Polyacrylonitrile (PAN Homopolymer), Poly(acrylonitrile-co-itaconic acid) (P(AN-co-IA)) and Poly(acrylonitrile-co-methacrylic acid) (P(AN-co-MAA)) based membranes were used.



## References

- [1] Sebesta F.J., Molt A., “ *Evaluation of PAN as a binding polymer for absorbers used to treat liquid radioactive wastes*” Department of nuclear chemistry- Czech Technical University in Prague.
- [2] ] Munch, H., Hansen, J. S., Pittelkow, M., Christensen, J.B., Boas, U., *Tetrahed. Lett.* (2008) 49, 3117
- [3] Van der Bruggen, B., Schaep, J., Wilms, D.; Vandecasteele, C. *J. Memb. Sci.* (1999) 156, 29.

# **Chapter 4**

## **Materials and Methods**

## 4.1 Computational details

The quantum mechanical calculations were carried out in the framework of DFT taking into account also the effect of the organic solvent used in the preparation of the membranes. The presented results were obtained using the NWChem code[1]. Different hybrid functionals have been used to describe hydrogen bonds [2-6]. Moreover, van der Wijst et al. [6]. showed that Becke-Perdew 86 and PBE functionals had good agreement with the post-HF and experimental hydrogen binding energies of DNA base pairs. The calculations of van der Wijst et al. [6] showed that the Becke-Perdew 86 and BPE functionals reproduced the binding energies better than the classical Becke-Lee-Yang-Parr (B3LYP) functional [7]. However, for the purpose of this work, the difference between the binding energies obtained using pure functional and B3LYP are acceptable. For this reason, the B3LYP potential and energy functional were used in this investigation. The calculations were performed using linear combinations of Gaussian-type atomic orbitals; Coulomb and exchange-correlation potentials were numerically integrated on an adaptive grid with medium accuracy. Triple- $\zeta$  atomic orbital basis set with a polarization function (6-311G\*) was employed for the atoms of the acrylic acid (AA) and MDA, whereas the 6-31G basis set was used for the remaining monomers of polymer models, that is acrylonitrile (AN). The energy convergence threshold was set to  $10^{-6}$  a.u. for the self-consistent field procedure, and the root-mean-square of the electron density was set to  $10^{-5}$  a.u. All molecular structures were fully optimized using analytical energy gradients with approximate energy Hessian updates. The optimization convergence was based on the maximum and root-mean-square gradient thresholds of  $(4.5 \text{ and } 3.0) \times 10^{-4}$  a.u., respectively, in conjunction with the maximum and root-mean-square of the Cartesian displacement vectors with thresholds of  $10^{-3}$ . The interaction energies were obtained at the same level of theory used for the optimizations of geometries. Since, the potential electronic surface of the supramolecular complexes considered in this work has many minima with energy lower than  $kT$  ( $T = 50^\circ\text{C}$  with  $k$  the Boltzmann constant), the Hessian calculations of the optimized geometries were performed only on those complexes that are significant for the purpose of the work, as shown below. The continuum conductor-like screening model proposed by Klamt and Schüürmann [10] was used to take into account the effects of the solvent on the binding energies. In general, continuum models to consider the solvent effects represent a good compromise between accuracy and computational costs. The dielectric constant needed

in the continuum conductor-like screening model of the solvent was set equal to 36.7, which corresponds to the dielectric constant of DMF employed in the preparation of the membranes. Moreover, both electrostatic and non-electrostatic contributions due to the solvent effect were taken into account in the calculation of the binding energies. The non-covalent intermolecular interaction energies were evaluated as the difference between the energy of the polymer model-MDA adduct and the energies of the single fragments. The basis set superposition error was therefore included in the calculation of binding energies according to the counterpoise method. When pure quantum mechanics approaches are used to evaluate bond energies or other molecular properties of macromolecules such as polymer chains, the choice of chemical models to describe polymers is crucial. It must be kept in mind that although DFT methodologies need computational efforts significantly lower than post-HF procedures, large models of polymers cannot currently be used. Consequently, in this work, molecular models of the modified PAN polymer were used. In particular, only the functional groups of polymer with a small part of backbone were taken into account. These structural models inevitably led us to neglect some noncovalent intermolecular interactions or other aspects, even if they may be irrelevant for the purpose of this thesis. However, experimental data and *had-hoc* tests were used to check the reliability of the polymer models and computational approach employed.

## 4.2 Evaluation of the binding energies of noncovalent interactions

The main binding energies are evaluated by building molecular models of the polymeric chains. In figure 4.1 are reported the molecular-scale models of modified polymer used in the calculations.



**Figure 4.1** Chemical structure of models representing the polymeric chains used for the preparation of membranes.

The nano-scale models used were two trimers simulating the composition of the polymeric chains that constitute the membranes. The first one is a trimer composed by 3 nitrile groups. This is a trimer of the polyacrylonitrile (PAN). The second one correspond to one trimer formed by 2 nitrile groups and one central acidic group, indicated with P(AN-co-AA). This second model is less probable along the PAN chains because the ratio estimated between acidic/nitrile groups in the polymer was around 0.1445. However, it is also important because the main interactions between target molecule and polymer were *via* the acidic functional group present in this trimer.

The bond between the carboxylic hydrogen and carbonyl group (Figure 4.2a) is the main noncovalent interaction experimented by the P(AN-co-AA) polymeric chains in addition to the electrostatic interactions between carboxylic hydrogen and nitrile (Figure 4b). Dispersion interaction among the triple bond of nitriles (Figure 4c) should have lower binding energy with respect to the above interactions and were not considered.

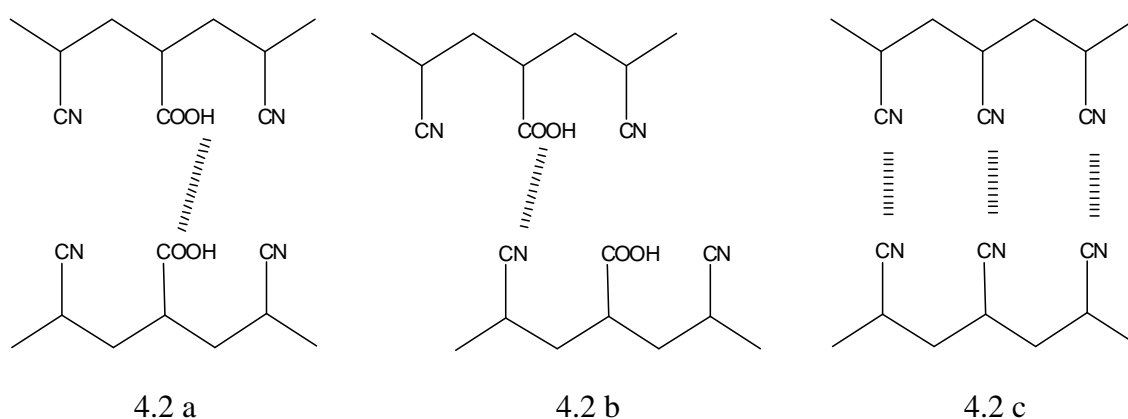


**Figure 4.2** Main noncovalent interactions between polymeric models.

Therefore, the CN-CN noncovalent bonds were not considered in this study. Concerning the main interactions among the template molecule and polymer models, they are those between the MDA amino group and carboxylic (Figure 4.3) or nitrile groups.

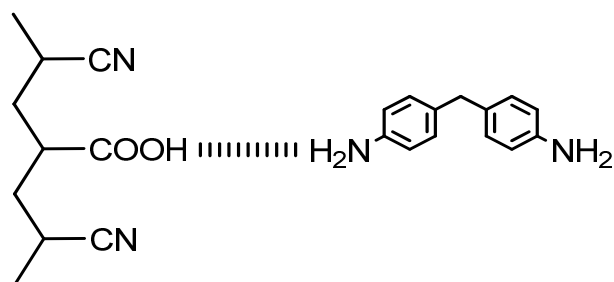


**Figure 4.3:** Main strong non-covalent interaction between the polymer and the target molecule.

However, as aforementioned, the last interaction should be considered to be lower than the first one. In Tables 4.3 and 4.4 are reported the obtained binding energies.

**Table 4.1:** Bond Energies (kilocalories per mole in vacuum computed at B3LYP/6-311\* Level of Theory.

| Complex  | $\Delta E_{\text{BSSE}}$<br>(kcal/mol) |
|--|--|
| ${}^0(\text{AN}_2\text{-co-AA})_2(\text{COOH}\cdots\text{CN})^{\text{io}}$         | -13,80                                 |
| ${}^0(\text{AN}_2\text{-co-AA})_2(\text{COOH}\cdots\text{COOH})^{\text{io}}$       | -15,50                                 |
| ${}^0(\text{AN}_2\text{-co-AA})_2(\text{COOH}\cdots\text{COOH})^{\text{oo}}$       | -12,67                                 |
| ${}^0(\text{AN}_2\text{-co-AA})_2(\text{COOH}\cdots\text{COOH})^{\text{ii}}$       | -9,49                                  |
| ${}^{90}(\text{AN}_2\text{-co-AA})_{2c}(\text{COOH}\cdots\text{COOH})^{\text{io}}$ | -20,91                                 |
| ${}^{90}(\text{AN}_2\text{-co-AA})_2(\text{COOH}\cdots\text{COOH})^{\text{io}}$    | -15,44                                 |
| MDA- (AN <sub>2</sub> -co-AA)  | -12,68                                 |
| MDA- (AN <sub>2</sub> -co-AA) <sub>2</sub>   | -25,56                                 |
| (AN <sub>2</sub> -co-AA - MDA) - (AN <sub>2</sub> -co-AA)                          | -12,70                                 |

**Table 4.2:** Bond Energies (kilocalories per mole in DMF computed at B3LYP/6-311\* Level of Theory.

| Complex   | $\Delta E_{\text{BSSE}}$<br>(kcal/mol) |
|---|--|
| ${}^0(\text{AN}_2\text{-co-AA})_2(\text{COOH}\cdots\text{CN})^{\text{io}}$                | -4,69                                  |
| ${}^0(\text{AN}_2\text{-co-AA})_2(\text{COOH}\cdots\text{COOH})^{\text{io}}$              | -7,82                                  |
| ${}^0(\text{AN}_2\text{-co-AA})_2(\text{COOH}\cdots\text{COOH})^{\text{oo}}$              | -3,88                                  |
| ${}^0(\text{AN}_2\text{-co-AA})_2(\text{COOH}\cdots\text{COOH})^{\text{ii}}$              | -3,40                                  |
| ${}^{90}(\text{AN}_2\text{-co-AA})_{2\text{c}}(\text{COOH}\cdots\text{COOH})^{\text{io}}$ | -14,25                                 |
| ${}^{90}(\text{AN}_2\text{-co-AA})_2(\text{COOH}\cdots\text{COOH})^{\text{io}}$           | -3,15                                  |
| MDA- (AN <sub>2</sub> -co-AA)   | -5,93                                  |
| MDA- (AN <sub>2</sub> -co-AA) <sub>2</sub>  | -14,70                                 |
| (AN <sub>2</sub> -co-AA - MDA) - (AN <sub>2</sub> -co-AA)                                 | -6,00                                  |

These values show that both in solvent and in vacuum the bond energies in the polymer-polymer and MDA-polymer adducts are comparable. The complexes with the prefix 0 are optimized starting from polymer model geometries having the carbon backbone parallel, whereas adducts with the prefix 90 are optimized structures starting from geometries with polymer backbone orthogonal. The structure forming a hydrogen bond or electrostatic interactions between carboxylic and nitrile groups is indicated, whereas the hydrogen bonds between two carboxylic groups are not explicitly reported. The orientations of the -CN groups located on the monomers near the acidic functional monomer are important because their orientation determines different steric hindrance with respect to the neighbouring carboxylic. In particular, the symbol “i” means that the -CN groups of one polymer fragment are directed inwards of the adduct, whereas the symbol “o” means that the -CN of one fragment are directed outwards of the complex. The  ${}^0(\text{AN}_2\text{-co-AA})_2(\text{COOH}\cdots\text{COOH})^{\text{ii}}$  adduct, reported in Figure 4.4 shows the lower binding energy both in solvent, -3.4 kcal/mol, and in vacuum, -9.5 kcal/mol.

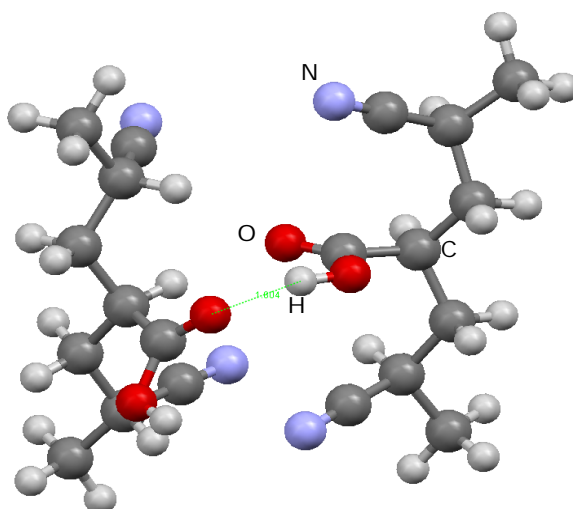


**Figure 4.4:** Optimised structure of the  ${}^0(\text{AN}_2\text{-co-AA})_2^{\text{ii}}$  adduct.

Furthermore, the binding energies of the more probable adduct,  ${}^0(\text{AN}_2\text{-co-AA})_2 - (\text{COOH}\cdots\text{CN})^{\text{i0}}$  reported in Figure 4.5, are -4.69 kcal/mol in solvent and -13.80 kcal/mol in vacuum.

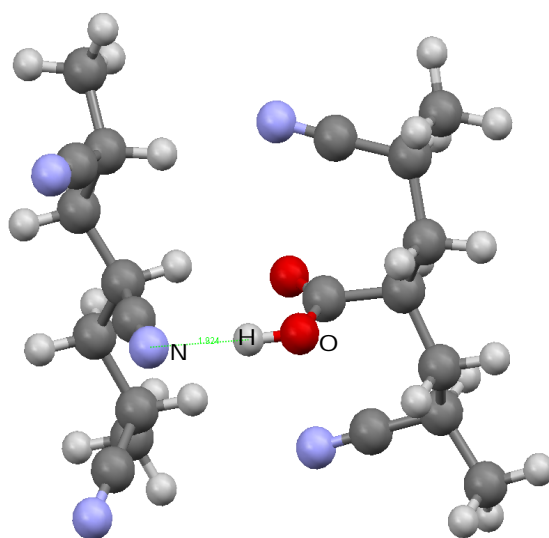


**Figure 4.5** Optimised structure of the more probable adduct,  ${}^0(\text{AN}_2\text{-co-AA})_2 - (\text{COOH}\cdots\text{CN})^{\text{i0}}$



Both binding energies are comparable to the energy of the noncovalent bond involved in the MDA-polymer complex shown in Figure 4.6.

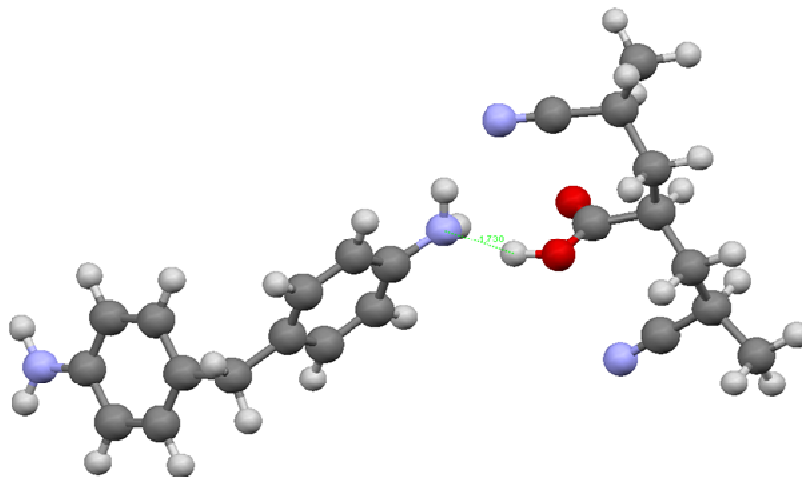


**Figure 4.6** Most probable interaction between the target molecule, MDA, and polymeric chain.

The  ${}^0(\text{AN}_2\text{-co-AA})_2(\text{COOH}\cdots\text{CN})^{\text{io}}$  adduct would be the more probable with respect to the  ${}^0(\text{AN}_2\text{-co-AA})_2(\text{COOH}\cdots\text{COOH})^{\text{io}}$  because the ratio between the AA and AN monomers in the copolymer, as previously indicated, is equal to 0.1445. The difference between the binding energy of  ${}^0(\text{AN}_2\text{-co-AA})_2^{\text{ii}}$  and  ${}^0(\text{AN}_2\text{-co-AA})_2^{\text{io}}$  complexes is due to the relative orientation of the -CN groups. In fact, these structures form similar hydrogen bonding, but, in the first case, the -CN groups of the fragments are directed inside the complex. This orientation increases the steric hindrance and decreases the correspondent binding energy. Instead, in the  ${}^0(\text{AN}_2\text{-co-AA})_2^{\text{io}}$  structure, the -CN groups of one fragment are directed inside, whereas the ones of the second fragment are directed outside. This orientation decreases the steric hindrance, and at the same time it creates an electrostatic long range interaction between the -CN groups of one fragment and the hydrogen atoms of the other fragment. In the case of the polymer-polymer complexes, the highest energies are obtained for the structure shown in Figure 4.7  ${}^0(\text{AN}_2\text{-co-AA})_{2c}^{\text{io}}$  are -14.3 kcal/mol in solvent and -20.9 kcal/mol in vacuum, whereas for the MDA-polymer complexes, the highest binding energy is obtained for the  $\text{MDA}\cdots(\text{AN}_2\text{-co-AA})_2$  (Figure 4.8) with energies equal to -14.7 and -25.6 kcal/mol in

solvent and in vacuum, respectively. For the  ${}^{90}(\text{AN}_2\text{-co-AA})_2(\text{COOH}\cdots\text{COOH})^{\text{i}0}$  adduct, the high values of binding energy are due to the formation of a cycle with two hydrogen bonds (Figure 7a), whereas the  $\text{MDA}\cdots(\text{AN}_2\text{-co-AA})_2$  binding energies are caused by the double hydrogen bond formed with two different fragments of the polymeric chains. Although these two interactions are favoured thermodynamically, the probability that these events take place during the formation of the membrane is lower than the probability of single hydrogen bond formation. The geometry optimization of the  ${}^{90}(\text{AN}_2\text{-co-AA})_{2\text{c}}^{\text{i}0}$  starts from polymer model geometries with orthogonal backbone. After full optimization, this polymer model arranges the carbon backbone in a parallel manner. A comparison between optimized and starting geometries revealed that the rotation of the polymer models from  $90$  to  $0^\circ$  is due to an arrangement of the polymer backbone in addition to the final rotation of the carboxyl groups. This arrangement can occur because in this study models of the polymer chain were considered. However, using very long chains, this particular arrangement may not occur. In addition, the formation of the cycle can occur.

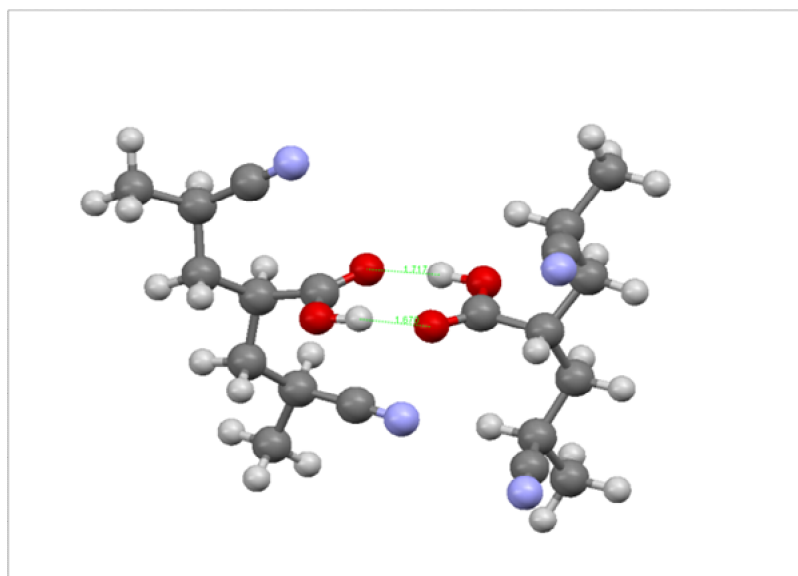


**Figure 4.7:** Optimized structure of the less probable adduct  ${}^{90}(\text{AN}_2\text{-co-AA})_2(\text{COOH}\cdots\text{COOH})_{2\text{c}}^{\text{i}0}$  having the highest binding energy.

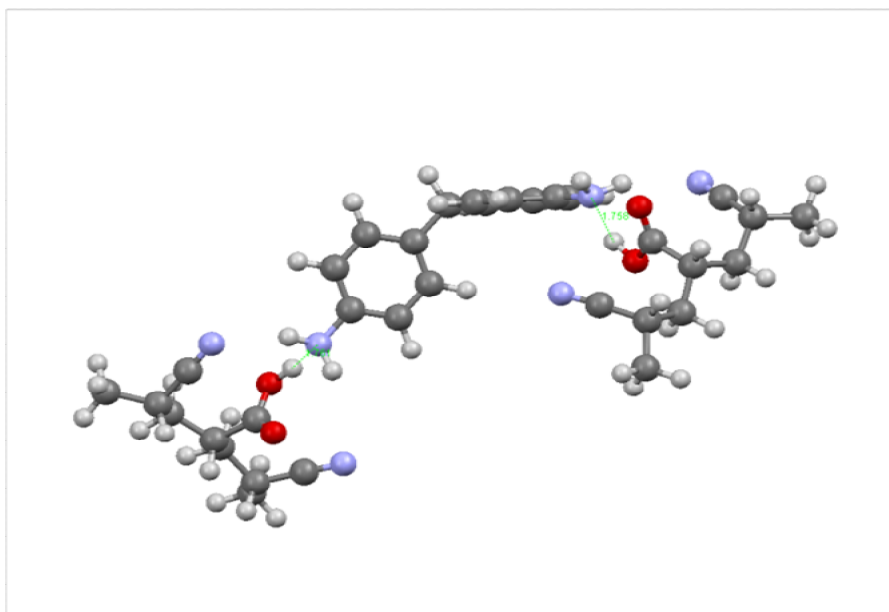


**Figure 4.8:** Optimized structure of MDA••• (AN<sub>2</sub>-co-AA)<sub>2</sub> having the highest binding energy.

when the -CN groups of the polymer model are direct outside the complex. Therefore, although the formation of a cycle with double hydrogen bonding is favoured thermodynamically, it should take place after the formation of a single hydrogen bond and then the subsequent rotation of carboxylic groups without the steric hindrance of -CN neighbour groups.

### **4.3 Causes controlling the affinity of the imprinted membranes toward the aminic compounds**

The computational results given above show that the target molecule in the casting solution can effectively bind to the carboxylic functional groups located on the polymer chains. This causes a greater availability of these functional groups once the MDA is removed from the formed membranes; otherwise, the carboxylic groups would interact by single hydrogen bonds among them (Figure 4.4) or with the -CN groups (Figure 4.5) giving the more probable structures (polymer + solvent). When the target molecules were added to the casting solution (polymer + solvent + MDA), some carboxylic groups will interact with the target molecule because the binding energies of MDA-polymer adducts are strong enough to break the bonds between polymer-polymer complexes. Once the template molecules were extracted, these functional groups remain free for

successive interactions with basic molecules. The sum of the free carboxylic groups, produced by the random arrangement of the polymeric chains and by the imprinting effect during the membrane preparation, increases the membrane affinity. Therefore, this work concludes that carboxylic groups of the copolymer, interacting via hydrogen bond and long-range electrostatic interactions with MDA, become free and more accessible in the imprinted membranes once the template and solvent are removed. For verifying this explanation, FT-IR spectra of membranes after target molecule extraction were done. To prepare the samples for the analysis, we dried all membranes in an oven at 90 °C overnight. In figure 4.9 is shown the spectra of blank membrane while the figure 4.10 the spectra of imprinted membrane after the extraction of target molecule.

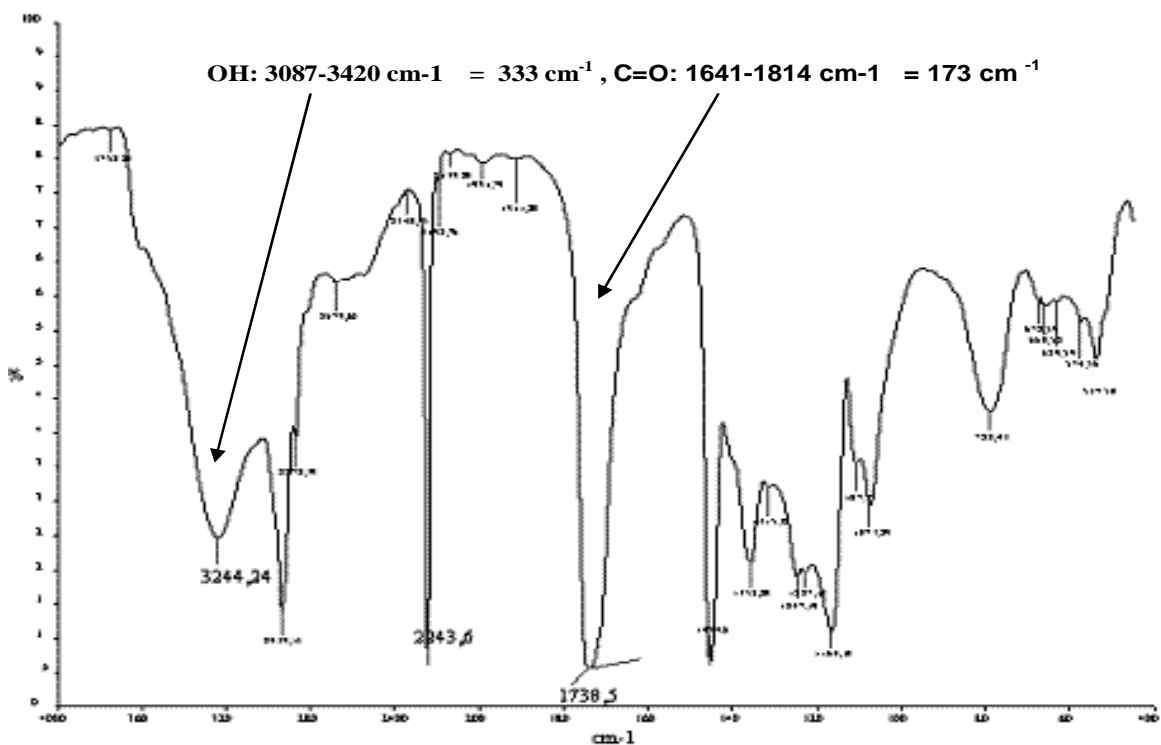


**Figure 4.9:** FT-IR spectra of blank membranes.

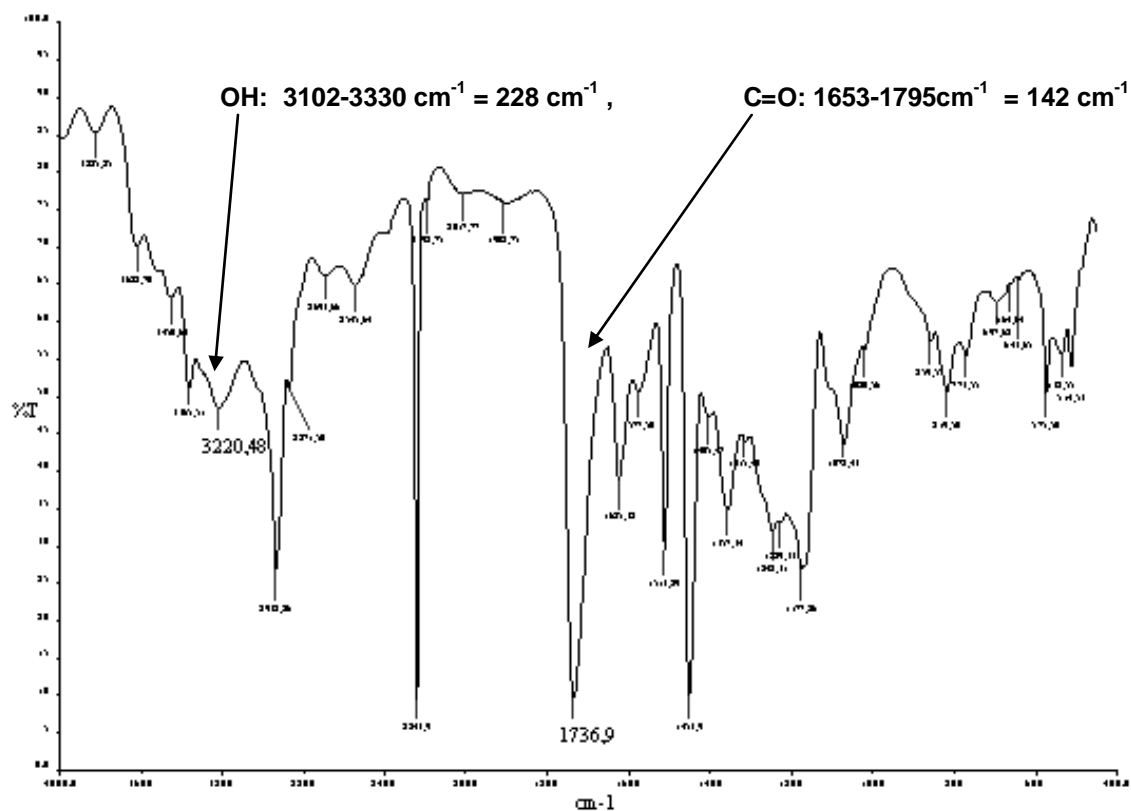


**Figure 4.10** FT-IR spectra of imprinted membranes after the template extraction.

From the analysis of the reported spectra, it was easy to note that the amplitudes of the C=O and OH typical stretching bands (C=O: 1653-1795  $\text{cm}^{-1}$  = 142  $\text{cm}^{-1}$ , OH: 3102-3330  $\text{cm}^{-1}$  = 228  $\text{cm}^{-1}$ ) in imprinted samples were thinner than in the blank samples (C=O: 1641-1814  $\text{cm}^{-1}$  = 173  $\text{cm}^{-1}$ , OH: 3087-3420  $\text{cm}^{-1}$  = 333  $\text{cm}^{-1}$ ). Larger IR stretching bands mean that more carboxylic groups of the polymer are interacting with each other. The comparison between the area of the C=O and OH peaks cannot be considered because they are not comparable. In fact, the casting solution of blank samples is formed by polymer and solvent; instead, in the imprinted casting solution, besides polymer and solvent, target molecule is also dissolved. Taking the same quantity of casting solutions, there will be less polymer in the imprinted solution with respect to the blank and, as a consequence, fewer carboxylic groups. The molecular weight of the target molecule is 198 g/mol, which means that at least five molecules of MDA may enter into the membrane pores according to the molecular weight cut-off measurements summarized in Table 4.3. Some rejection tests were carried out using some dyes. We observed that for the rose of Bengal the rejection was 92%. This result

allows us to estimate the molecular weight cut-off of the membranes around the molecular weight of the dye (1000 Dalton).

**Table 4.3:** Dyes used, molecular weight and rejections results in buthanol.

| <b>Dye</b>       | <b>Molecular weight<br/>(g/mol)</b> | <b>Rejection (%)</b> |
|------------------|-------------------------------------|----------------------|
| Methyl Orange    | 327                                 | 15                   |
| Bromothymol Blue | 624                                 | 60                   |
| Rose of Bengal   | 973                                 | 92                   |

The correlation between weight and molecular effective size cannot be rigorous and accurate [14] especially for small molecules. Therefore, the effective diameters of the rose Bengal, MDA, and aniline were calculated. The effective diameter is defined as the weighed average projection on the membrane surface of the maximum and minimum molecular sizes. The molecular geometries were optimized using the same level of theory described in the Computational Details. Concerning the influence of the molecular sizes on the effectiveness in separation of the imprinted membranes, the ratio between the molecular dimensions of impurities, dye and the membrane pore size was also studied theoretically and experimentally. The effective diameter of Rose of Bengal MDA and MDA aniline were calculated by means also of quantum mechanics calculations and homemade algorithm and reported in table 4.4. In this Table, the relative above cross section ratios were therefore presented. This analysis concluded that the ratio between the effective diameter of Rose of Bengal (19.20 Å ) and MDA (13.98 Å) was 1,3 which means that the average pore size must considered between 19.0 Å and 13.0 Å. The average pore size of the membranes is almost similar to the dimensions of MDA.

**Table 4.4:** Effective diameter and other useful values of the Rose of Bengal, MDA and aniline.

| Molecule            | $D_{\text{eff}}$ (Å) | $D_{\text{RB}}/D_{\text{eff}}$ | Cross-section ratio |
|---------------------|----------------------|--------------------------------|---------------------|
| Aniline             | 9.872                | 1.954                          | 3.817               |
| MDA                 | 13.980               | 1.380                          | 1.903               |
| Rose of Bengal (RB) | 19.287               | 1.000                          | 1.000               |

The values of table 4.4 show that less than two molecules of MDA could pass through the pores of the membrane, whereas approximately four molecules of aniline can cross the membrane through its pores. Considering the values of Table 4 and the fact that a molecule should have the time to bond with the free and more available carboxylic groups in the pores of the membrane one might predict that the aniline should be retained less than MDA by both blank and imprinted membranes because the average size of the membrane pores is markedly larger than the size of the aniline molecule; therefore, the effect due to the free carboxylic groups inside the pores should be less pronounced. It is important to emphasize that the last aspect is related only to the average size of the membrane pores formed according to the dry-wet phase procedure by which the membranes for nanofiltration are usually prepared. In figure 4.11 is represented an ideal representation of the membrane pores. According to the results present in table 4.4 and the theoretical binding energies, the aniline feels the interaction of acidic groups but, due to the large pore size, the high pressure (around 6 bar) drags the molecule through the membranes. On the other hand, MDA has an effective diameter almost the same of the pores (Table 4.4) and it is able to interact with acidic groups in the pore walls even at high pressures. The influence of the solvent on the proposed mechanism is under investigation (*work in progress*).

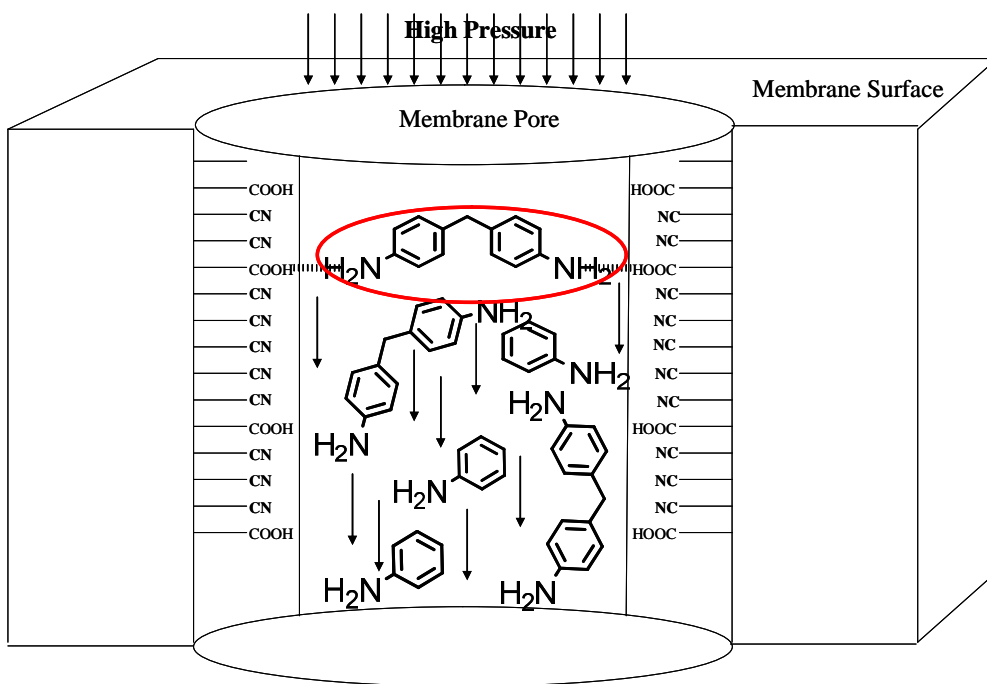


**Figure 4.11:** Ideal representation of a possible homogeneous membranes pore configuration.

Hence, in our opinion it would be crucial to dissociate the effect caused by the imprinting from that due to the simple size exclusion by the membrane pores. In other words, this second aspect is not directly linked to the imprinting of membranes. If the effective diameter of the target molecule is not similar to the average pore size of the membrane the high pressure confers to the target molecule a elevated linear moment dragging it trough the pores and avoiding the possible interactions with acidic functional groups.



## 4.4 Development of molecularly imprinted membranes for selective recognition of primary amines in organic medium[15]

### 4.4.1. Preparation and characterization of polymers

Different acrylic co-polymers were prepared *via* the water-phase precipitation copolymerization method. The experimental fact of this method is that monomers and initiators were all water soluble. Thus, the polymerization reaction took place in aqueous media. On the other hand, since the polymer formed was not soluble in water precipitated from the aqueous phase and was easily take apart by a simple filtration. The rest of the components of the reaction (un-reacted monomers and initiators) were removed during the repeated washing steps with fresh water.

FT-IR spectra of all polymers were done in order to ensure the presence of acidic groups into the PAN polymeric chains. In figure 4.12 is easily visible that all spectra present 3 common peaks: a peak around  $2244\text{ cm}^{-1}$  caused by the stretching vibrations of (C-N) belonging to nitrile groups; another peak around  $1454\text{ cm}^{-1}$  produced by the bending vibrations of the different  $\text{C}_{\text{sp}^3}\text{-H}$  and finally a weak peak at about  $2940\text{ cm}^{-1}$  due to the stretching vibrations of  $\text{C}_{\text{sp}^3}\text{-H}$ . The common peaks indicate that polymers are composed by hydro-carbonated chains having nitrile groups. The observation of the copolymers spectra clearly evidences a new peak at  $1732\text{ cm}^{-1}$  produced by the stretching of carbonyl group (C=O) characteristic of carboxylic acids. There is also visible a quite wide and large peak in the range going from  $3700$  to  $3400\text{ cm}^{-1}$  approximately created by the stretching vibration of hydroxyl group (O-H) belonging to carboxylic acids present in the polymer forming the membranes. The large extension of the peak is due to the hydrogen bond created by acidic groups.

Spectroscopic results confirm the presence of acidic moieties into the polyacrylonitrile chains because eventual monomers un-reacted are soluble in water and, like mentioned before, would have been removed during the washing step.

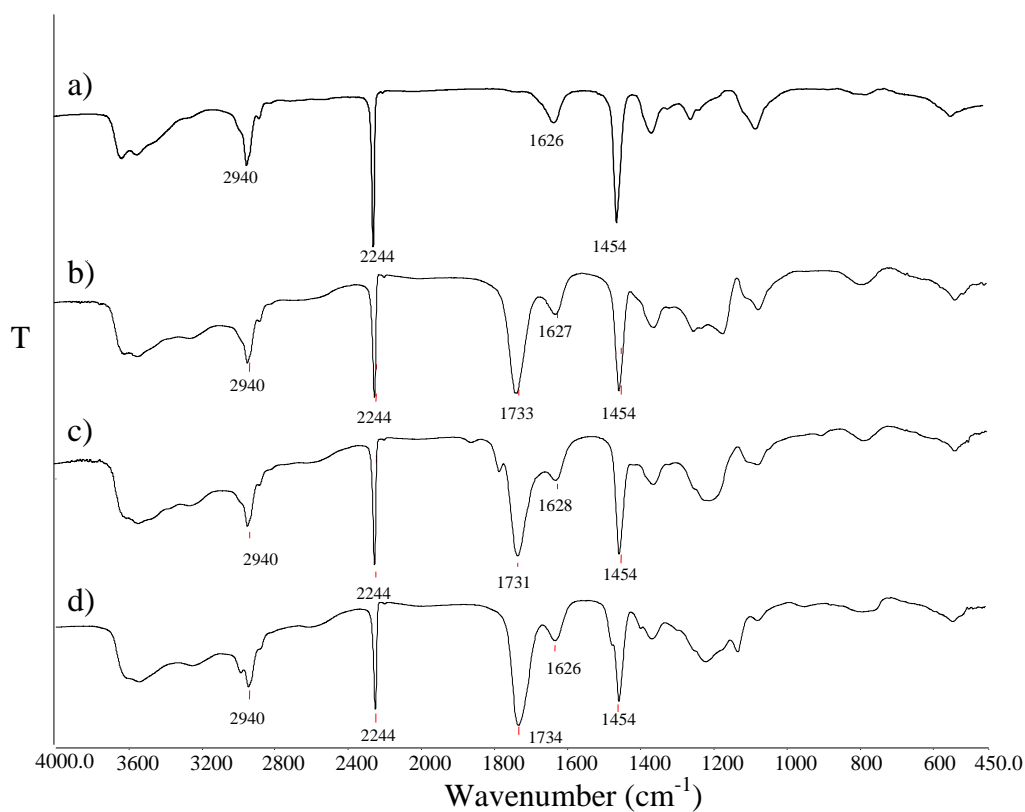


**Fig 4.12:** FT-IR spectra of PAN homopolymer (a); PAN-co-AA (b); PAN-co-IA (c) and PAN-co-MAA (d).

Table 4.5 shows the polymerization yield, the intrinsic viscosity and average molecular weight of the synthesised polymers.

**Table 4.5:** Polymerization yield, intrinsic viscosity and average molecular weight of the synthesised polymers.

| Polymer      | Yield (%) | $[\eta]$ (ml/g) | $M_v$ ( $\times 10^{-3}$ g/mol) |
|--------------|-----------|-----------------|---------------------------------|
| PAN          | 82        | 279             | 167                             |
| P(AN-co-AA)  | 64        | 319             | 199                             |
| P(AN-co-MAA) | 72        | 413             | 279                             |
| P(AN-co-IA)  | 60        | 271             | 169                             |

#### 4.4.2 Preparation and characterization of membranes

The utilization of dry-wet process permitted to obtain dense films prepared with the scope of being used as absorbers devices for the specific recognition of MDA in organic medium. SEM analysis of these membranes evidenced that there were not significant differences in morphology between blank and imprinted membranes and between membranes prepared with the different copolymers. The common particularity showed by all of membranes prepared, in terms of morphology, was the elevated dense structure. Figure 4.13 reports SEM images of the surface and the cross-section of P(AN-co-AA) based membranes.

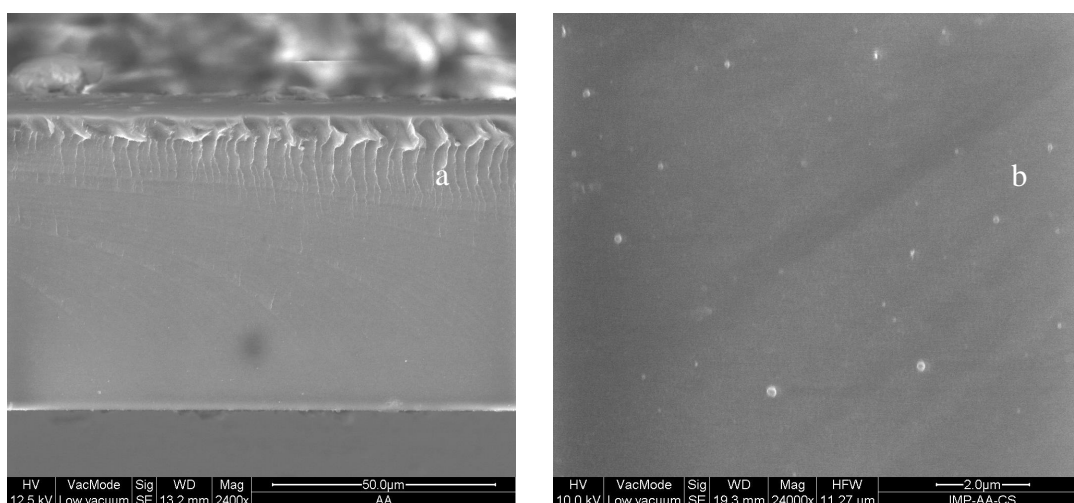


**Fig. 4.13:** SEM images of cross-section (a) and surface (b) of imprinted membranes prepared with P(AN-co-AA).

Membrane permeability in water and in IPA is reported in table 4.6.

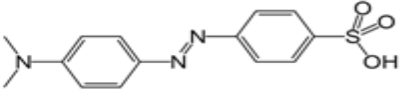
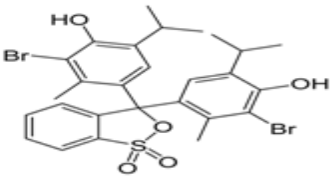
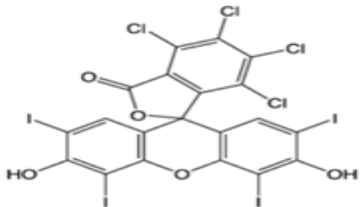
**Table 4.6:** Permeability in water, IPA, and thickness of the membranes prepared with the different polymers.

| <b>Membranes</b>          | <b>Water Permeability<br/>(L/h m<sup>2</sup> bar)</b> | <b>Permeability<br/>In IPA<br/>(L/h m<sup>2</sup> bar)</b> | <b>Thickness<br/>μm</b> |
|---------------------------|---|--|-------------------------|
| Blank<br>PAN              | 11.5±2.0  | 4.9±0.8  | 100                     |
| Imprinted<br>PAN          | 10±1.5  | 4.2±0.5  | 115                     |
| Blank<br>P(AN-co-AA)      | 15.5±1.0  | 3.1±1.0  | 110                     |
| Imprinted<br>P(AN-co-AA)  | 13±1.5  | 2.3±0.5  | 120                     |
| Blank<br>P(AN-co-MAA)     | 10±0.7  | 3.15±1.  | 115                     |
| Imprinted<br>P(AN-co-MAA) | 9.5±0.7   | 2.1±0.5  | 125                     |
| Blank P(AN-co-IA)         | 8.5±1.5   | 3.95±1.0   | 90                      |
| Imprinted<br>P(AN-co-IA)  | 11.5±2.1  | 3.65±0.63  | 90                      |

Data of table 4.6 shows that values were in the typical nanofiltration range although in the case of IPA they were sensitively lower. No significant differences were observed between blank and imprinted membranes and before and after template removal from MIMs.

The experimental determinations of the molecular weight cut-off performed both, in IPA and buthanol gave the same results. Chemical structure and molecular weight of the different used dyes as well as rejection are shown in table 4.7. Because of the similar permeability of imprinted and blank membranes, experiments were carried out only using blank samples. On the basis of the rejection results the molecular weight cut-off of the tested membranes was estimated to be around 1000 dalton.

**Table 4.7:** Structure, molecular weight and rejection of the different used dyes.

| Dye              | Chemical structure  | Mw (Dalton) | Rejection (%) |
|------------------|---|-------------|---------------|
| Methyl Orange    |  | 327         | 15            |
| Bromothymol Blue |  | 624         | 40            |
| Rose of Bengal   |  | 973         | 92            |

#### 4.4.3 Binding experiments.

Binding tests were performed in order to investigate the recognition properties of P(AN-co-AA) based membranes towards the target molecule. First studies were carried out to study the influence of the initial concentration of MDA in solution on the sorption capacity of imprinted and blank membranes. Like figure 4.14 shows As higher was the initial concentration of MDA during binding experiments, higher was the sorption capacity of both blank and imprinted membranes. This behaviour can be explained by the fact that the augment of initial MDA concentration probably increased the total amount of template available for the interaction with the acidic groups of polymeric chains when it was in contact with the membrane. The highest binding capacity values were observed during experiments with 10 mg/L of initial MDA concentration, being 5  $\mu\text{mol/g}_{\text{memb}}$  and 2.4  $\mu\text{mol/g}_{\text{memb}}$  the amount of MDA retained by imprinted and blank membrane, respectively. The difference between the MDA retained by the imprinted and the blank membrane gave the specific binding capacity of the MIM that was 2.6  $\mu\text{mol/g}_{\text{memb}}$ .

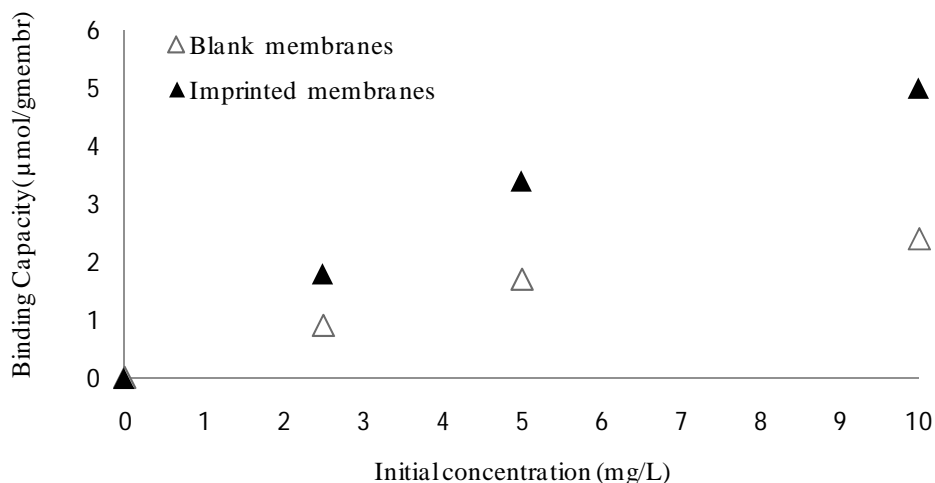


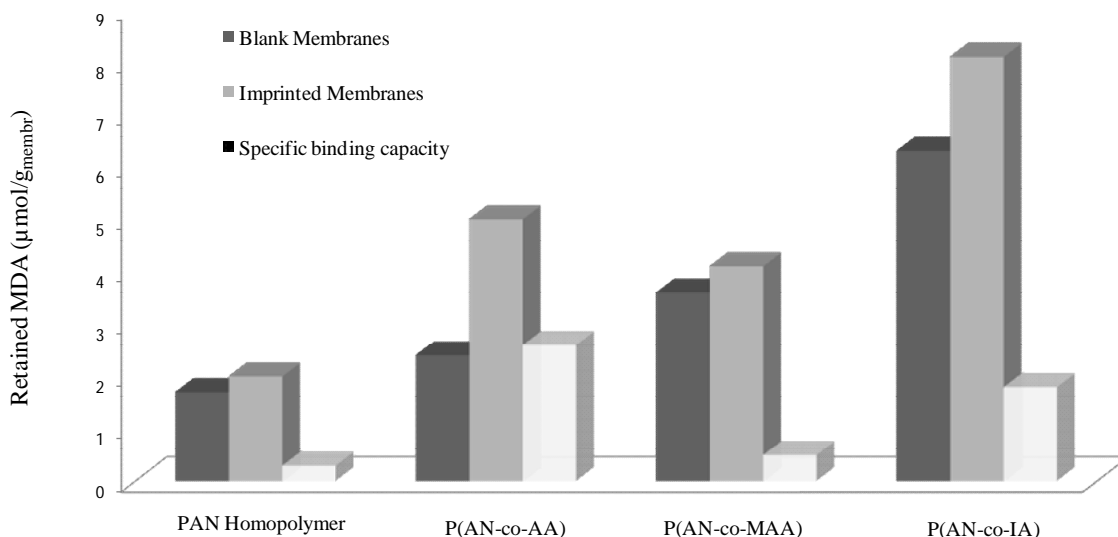
**Fig. 4.14:** MDA retention by P(AN-co-AA)-MDA imprinted and blank membrane after filtration experiments in IPA at different initial MDA concentration.

The selective properties of P(AN-co-AA)-MDA imprinted membranes were evaluated performing binding tests using EDA and Aniline. The initial concentration of these compounds was 10 mg/L. The utilization of this concentration in selectivity studies is due to the maximum overall sorption capacity showed by the membranes at this operation conditions. Results, compared with those obtained for the template, are reported in table 4.8 As it can be seen, membranes were completely selective between MDA and aniline, showing null sorption capacity towards aniline. Blank membranes exhibited almost similar retention capacity for EDA and MDA while imprinted membranes were able to discriminate between template and its structural analogue even though EDA is almost identical to MDA, having only one CH<sub>2</sub> group more. The selectivity factor *MDA/EDA* was 1.6.

**Table 4.8** : Binding capacities and selectivity factor of P(AN-co-AA) based membranes

| Analyte | Membrane      | Binding capacity                           | Selectivity factor |
|---------|---------------|--|--------------------|
|         |               | ( $\mu\text{mol}/\text{g}_{\text{memb}}$ ) | ( $\alpha$ )       |
| MDA     | Blank         | 2.3 $\pm$ 0.2                              | 1.6                |
|         | MDA-Imprinted | 4.7 $\pm$ 0.2                              |                    |
| EDA     | Blank         | 2.0 $\pm$ 0.2                              | 1.6                |
|         | MDA-Imprinted | 2.9 $\pm$ 0.1                              |                    |
| Aniline | Blank         | No retention                               | Completely         |
|         | MDA-Imprinted | No retention                               | Selective          |

Molecular recognition properties toward MDA of membranes prepared with PAN homopolymer, P(AN-co-IA) and P(AN-co-MAA) copolymers were also evaluated. Binding experiments were done with blank and imprinted membranes and following the same procedure previously described with 10 mg/L of initial MDA concentration. Results, reported in Figure 4.15 were compared with those obtained with the previously studied P(AN-co-AA)-imprinted and blank membranes.

**Fig. 4.15:** MDA retention and specific binding capacities of the membranes prepared using PAN and the different acrylic copolymers.

PAN homopolymer based membranes showed the lowest and non-specific MDA retention. Among the copolymers, P(AN-co-MAA) imprinted membrane exhibited the lowest specific binding capacity toward MDA ( $0.5 \mu\text{mol/g}_{\text{memb}}$ ). It is important to remark that both, imprinted and blank P(AN-co-IA) based membranes showed high MDA retention but the specific binding capacity of imprinted membrane was lower ( $1.8 \mu\text{mol/g}_{\text{memb}}$ ) than that one exhibited by P(AN-co-AA) membrane ( $2.6 \mu\text{mol/g}_{\text{memb}}$ ) previously discussed. On the basis of the experimental results it was concluded that P(AN-co-IA) –based membranes exhibited an elevated non specific sorption.

In another study buthanol permeability of P(AN-co-AA) based membranes was also determined. The data are shown in table 4.9. Both values of blank and imprinted membranes permeability values are of 1 and  $0.8 \text{ L/m}^2 \text{ h bar}$  respectively, are in the typical nanofiltration ranges.

**Table 4.9:** Permeabilities in buthanol of prepared (P(AN-co-AA) based membranes.

| Membrane  | $L_p$ ( $\text{L/m}^2 \text{ h bar}$ ) in buthanol |
|-----------|--|
| Imprinted | $0.8 \pm 0.2$                                      |
| Blank     | $1 \pm 0.1$  |

Binding tests were also performed in buthanol in order to study the influence of a less polar binding solvent on the membranes recognition properties.

Results of binding experiments reported in figure 4.16 showed that the prepared membranes retained a different amount of MDA. In particular, blank membrane exhibits a binding capacity as low as  $2.0 \mu\text{mol/g}_{\text{memb}}$ . The imprinted membrane shows a much higher retention,  $8.6 \mu\text{mol/g}_{\text{memb}}$ . Therefore, the difference between the imprinted and blank membrane,  $6.6 \mu\text{mol/g}_{\text{memb}}$  gives the specific binding capacity due to the imprinting phenomena. This values are quite better than those obtained in IPA. ( See binding tests in IPA above). The utilization of a less polar solvent during binding experiments improved the molecular recognition of the prepared membranes.



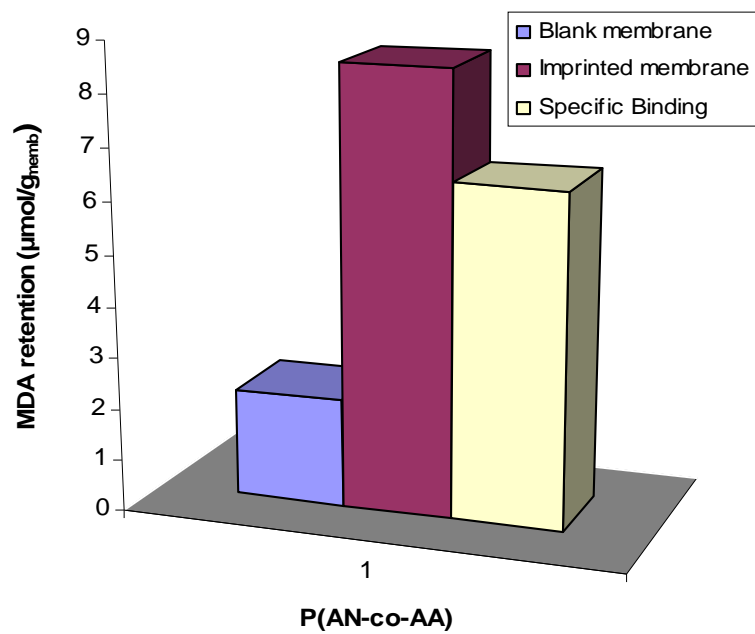


**Figure 4.16:** Retained MDA and specific binding capacity of blank and MDA-imprinted membranes in buthanol.

## References.

- [1] Straatsma, T. P., Apra, E., Windus, T. L., Dupuis, M. E., Bylaska, J., de Jong, W., Hirata, S., Smith, D. M., Hackler, A. M., Pollack, T. L., Harrison, R. J., Nieplocha, J., Tipparaju, V., Krishnan, M., Brown, E., Cisneros, G., Fann, G. I., Fruchtl, H., Garza, J., Hirao, K., Kendall, R.; Nichols, J. A.; Tsemekhman, K.; Valiev, M.; Wolinski, K.; Anchell, J.; Bernholdt, D.; Borowski, P.; Clark, T.; Clerc, D.; Dachsel, H.; Deegan, M.; Dyall, K.; Elwood, D.; Glendening, E.; Gutowski, M.; Hess, A.; Jaffe, J.; Johnson, B.; Ju, J.; Kobayashi, R.; Kutteh, R.; Lin, Z.; Littlefield, R.; Long, X.; Meng, B.; Nakajima, T.; Niu, S.; Rosing, M.; Sandrone, G.; Stave, M.; Taylor, H.; Thomas, G.; van Lenthe, J.; Wong, A.; Zhang, Z. NWChem, A Computational Chemistry Package for Parallel Computers, version 5.1.1; Pacific Northwest National Laboratory: Richland, WA, 2005.
- [2] Fonseca Guerra, C.; Bickelhaupt, F. M.; Snijders, J. G.; Baerends, E. J. J. *Am. Chem. Soc.* 2000, 122, 4117.
- [3] Zhao, Y.; Truhlar, D. G. *J. Phys. Chem. A* 2005, 109, 5656.
- [4] Leng, Y.; Krstic, P. S.; Wells, J. C.; Cummings, P. T.; Dean, D. J. *J. Chem. Phys.* 2005, 122, 244721.
- [5] De Luca, G.; Tocci, E.; Drioli, E. *J. Mol. Struct.* 2005, 739, 163.
- [6] Van der Wijst, T.; Fonseca Guerra, C.; Swart, M.; Bickelhaupt, F. M. *Chem. Phys. Lett.* 2006, 426, 415.
- [7] Grimme, S. *J. Comput. Chem.* 2006, 27, 1787.
- [8] De Luca, G. NanoMemCourse EA3 (Nano-Structured Materials and Membranes in the food Industry) Proceedings 2010, A24/L24.
- [9] Klamt, A.; Schüürmann, G. *J. Chem. Soc., Perkin Trans.* 1993, 2, 799.
- [10] Tomasi, J.; Mennucci, B.; Cammi, R. *Chem. Rev.* 2005, 105, 2999.
- [11] De Luca, G.; Mineva, T.; Russo, N.; Sicilia, E.; Toscano, M. *Continuum Dielectric Models for the Solvent and Density Functional Theory: The State of the Art. In Recent Advances in Density Functional Methods. Part II*; Chong, D. P., Ed.; World Scientific Publishing: Singapore, 1997; Chapter 3.

- [12] Barone, V.; Cossi, M.; Tomasi, J. *J. Chem. Phys.* 1997, 107, 3210.
- [13] Simon, S.; Duran, M.; Dannenberg, J. J. *J. Chem. Phys.* 1996, 105, 11024.
- [14] L. Braeken, R. Ramekers, Y. Zhang, G. Maes, B. Van der Bruggen, C. Vandecasteele. *Desalination*. (2006) 199, 245.
- [15] García Del Blanco, S., Donato, L., Drioli, E., *Sep. Purif. Technol.* (2011).
- Accepted for publication.**

# **Conclusions and further works**

To understand the causes, at molecular level, determining the increase of affinity of imprinted polymeric membranes towards the 4,4-methylenedianiline dissolved in buthanol, we performed a computational and experimental investigation during this PhD thesis. The attention was focused on this kind of separation because works on this issue are not numerous at all. We performed accurate quantum mechanics calculations in the framework of Functional Density Theory (DFT) to evaluate the main noncovalent interactions between polymer and target molecule using nano-scale models to represent the polymeric chains. As a result of these calculations, we established that both in the solvent used for the membranes preparation (DMF) and in vacuum the interactions between polymeric chains and those between MDA and polymeric chains are globally comparable (in competition). Thus, the template molecule in the casting solutions allows to break some bonds involved between the polymer chains. In blank samples of casting solution the MDA is not present, hence the above competition cannot occur. Once formed the imprinted membrane, the subsequent extraction of template molecule causes an increasing of availability of free acidic groups that subsequently can interact with MDA during the nanofiltration. Therefore, the increased availability of the carboxylic functional groups, located along the polymer chains, is one of the driving forces for the increased affinity of the membranes to aromatic amine molecules or in general to amines with comparable dimension of MDA. In particular, the enhancement of the free carboxylic groups in the imprinted membranes is caused by the presence of the basic target molecule in the casting solution during the membrane preparation. In fact, the free acid groups, produced by the random arrangement of the polymeric chains, are added to those produced by the imprinting effect. This increases the affinity of these kinds of MIMs. This is one of the causes controlling the increasing of affinity of the imprinted samples. In fact, the average size of the membrane pores must always be kept in mind in these separations, although this general factor is intrinsic to the (dry-wet phase) procedure by which membranes for nanofiltration are always prepared.

Nanofiltration and noncovalent Molecular Imprinted Membranes are well established techniques in the molecular separations area. If the average pore size is markedly larger than the effective size of the target molecule, increasing the pressure, the imprinting phenomena loses their capacity to absorb target molecules. This phenomena is caused because interactions governing the membrane affinity versus the target molecule are purely noncovalent as demonstrated in our paper (*J. Phys. Chem B* (2011), 115, 9345).

Using the quantum mechanics modelling we are studying the possibility to synthesize a particular P(AN-co-AA) co-monomer in which the acidic functional groups, able to interact via hydrogen bond with MDA, be intercalated in the acrylonitrile chain so that they could interact more exactly with the two amino groups of the MDA hosting the molecule. Being a random polymerization of AN and the acidic group (AA), the challenge is to know the ratio between AN/AA groups to mix during the random synthesis to create a co-monomer with the acidic groups in a configuration able to host spatially one molecule of MDA, that is interact more exactly with the two amino groups.

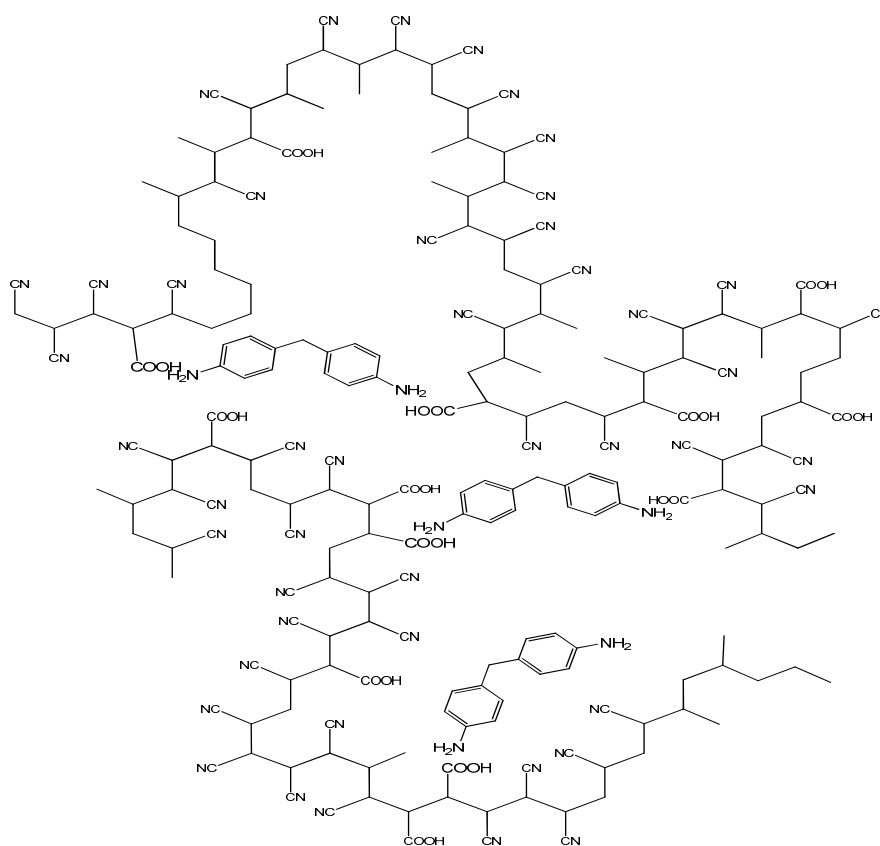


**Figure C.1:** Not homogeneous pore configuration with the MDA molecules.

As a further work, we would like to understand how the molecular size and the binding energies combine to give a specific molecular recognition. Figure C.1 shows a schematic representation of membrane with not homogeneous pore configuration with

the molecules of MDA interacting with carboxylic groups of the polymer. As shown in this Figure the aforementioned quantities (molecular size and the binding energies) should play a crucial role in the recognition of the target molecules in addition to the flexibility of the polymeric backbone. In other words, how these two quantities can allow the recognition of a particular molecule and not rather a class of molecules. By this way we expect that the molecular recognition will be widely higher than that found in this work thesis.

# Proceedings



**\* NF molecularly imprinted membranes for removal of genotoxic substances from organic solvents.**

Samuel García Del Blanco, Laura Donato, Giorgio De Luca, Enrico Drioli.

*ITM-CNR, Via P. Bucci Cubo 17/C – University of Calabria, 87030 Rende (CS) – Italy.*

Third International Conference on Organic Solvent Nanofiltration, Imperial College London, UK, 13-15 September 2010. **Poster presentation.**

**\* Molecular recognition performance of new 4,4'-methylenedianiline imprinted membranes.**

L. Donato<sup>1</sup>, Samuel García Del Blanco<sup>1,2</sup>, F. Tasselli<sup>1</sup>, G. De Luca<sup>1</sup>, E. Drioli<sup>1,2</sup>

*1-Institute on Membrane Technology, via P. Bucci Cubo 17/C, 87030 Rende, Italy.*

*2-Department of Chemical Engineering and Materials, University of Calabria, 87030 Rende, Italy.*

International Conference On Membranes and Membranes Processes (ICOM 2011) 23-29 July 2011, Asmterdam, The Netherlands. **Poster presentation.**

**\* Preparation and Characterization of Non-Covalent Molecularly Imprinted membranes for Application in Solid-Phase Extraction.**

Laura Donato<sup>1</sup>, Franco Tasselli<sup>1</sup>, Samuel García del Blanco<sup>1,2</sup> Enrico Drioli<sup>1,2</sup>

*1-Institute on Membrane Technology, via P. Bucci 17/C 87036 Rende, Italy*

*2-Department of Chemical Engineering and Materials, University of Calabria 87036 Rende Italy.*

4th Graduate Student Symposium on Molecular Imprinting. Imperial College- London, UK 28- 30th September, 2011. **Poster presentation.**

# **Publications**

\* G. De Luca, L. Donato, S. García Del Blanco, F. Tasselli, and E. Drioli, **On the Cause of Controlling Affinity to Small Molecules of Imprinted Polymeric Membranes Prepared by Noncovalent Approach: A Computational and Experimental Investigation**, *J. Phys. Chem B* (2011), 115, 9345-9351.

\* S. García Del Blanco, Laura Donato and Enrico Drioli, **Development of molecularly imprinted membranes for selective recognition of primary amines in organic medium**, *Sep. Purif. Technol.* (2011). Accepted for publication.